Lateral Load Capacity of Model Piles on Cohesion-less Soil at 3D Pile Spacing

Babu S Chawhan[1*], Gururaj Vijapur[2], Girish K H[3], Siddangouda Patil[4], Shreepad Desai[5], Yogeendra R Holebagilu[6]

[1,2,5] Department of Civil Engineering, Government Engineering College, Haveri, Karnataka, India

[3]Department of Geology, Government Engineering College, Haveri, Karnataka, India

[4,6] Department of Civil Engineering, Government Engineering College, Huvinahadagali ,Bellary, Karnataka, India

ABSTRACT

This paper presents the results of analysis of laterally loaded stainless steel pipe piles embedded in multilayered cohesion-less soil. An experimental investigation on model piles had been carried out using stainless steel pipe pile with outer diameter of 24mm and inner diameter of 20mm with different slenderness ratio of 25, 30 and 38 in a multilayered cohesion-less soil. In first case, a loose layer is maintained between the dense layers with H/D ratio of 0.50 and in second case, only dense cohesion-less soil layer of H/D ratio 0.0 is maintained with the depth of 0.0m. Where, H is the depth of middle cohesion-less soil layer and D is the embedment depth of pile of different slenderness (L/d) ratio of 25, 30 and 38. The experimental results of first case and second case show that the lateral load–lateral displacement response depends on the slenderness ratio of the piles. The experimental program was further verified by a two dimensional finite-element technique. The experimental results were compared with numerical analysis and are in a close agreement.

Keywords: *Stainless steel, Finite element analysis, Lateral load capacity, Lateral displacement, Slenderness ratio.*

1. Introduction

The deformation behaviour of a single pile subjected to horizontal loads is a well-known method for modelling the soil reaction-lateral displacement (p-y) approach. To understand the deformation behaviour of each of the pile in a pile group, subjected to lateral loads or a combination of vertical and lateral loads, it is very essential to know the clear idea of the deformation behaviour of single piles of similar batter under lateral load cases. The behaviour of a single pile is controlled by it's location in the group and it's pile head fixity. The lateral resistance of a pile is influenced by the "shadowing effects" as explained by Brown et al. [21] for both the horizontal subgrade modulus and the ultimate lateral resistance in a group are decreased because of the overlapping of the stress zones in the close soil. In fixed-head pile group, bending moments and shear forces are developed at the pile heads and surrounded by the pile cap. The later were negligible under vertical forces within the piles, which were transfer to skin and tip resistances along each pile. The importance of such limit was studied for both battered and driven pile group in loose sand by McVay et al. [17] to facilitate the characterize both the vertical and horizontal behaviours of piles is essential to model a group response subjected to lateral loads.

Few methods were proposed and implemented to models of lateral group response by Focht and Koch [25] proposed a method that combines the soil reaction-lateral displacement (p-y) approach for single pile by Poulos [22] approach for pile group. They have developed a group amplification procedure based on pile group field tests. Davisson [27] modified the elastic solution to account the non-linearity using yield factors and the modulus of subgrade reaction approach was extended to account for the soil non-linearity. Nak-Kyung et al.[14] have observed that, testing of the pile embedded in Nak-Dong river sand, located in south Korea, under monotonic lateral loadings. The lateral resistance of piles, effect of the installation methods and pile head restraint conditions were studied. The lateral load is highest in the free head condition and it decreases as the depth increases. Prakash and kumar [18] concluded that, the modulus of subgrade reaction depends on the relative density of sands and depth of the ground water-table. Rao et al. [16] concluded that, results of the lateral load capacity of pile groups depends mainly

211

on the rigidity of pile soil system for different configurations of piles within the group. Chandrasekaran et al. [8] investigated the effects of pile spacing, number of piles, embedment length and configurations on pile-group interaction, the experimental results found that the lateral capacity of piles in nine pile group at three-diameter spacing is about 40% less than that of the single pile and causes 20% increase in the maximum bending moment when compared with a single pile. Salini and Girish [10] concluded the lateral-load capacity of pile group increases as the density of sand increases for the same slenderness ratio. The lateral-load capacity increases with increase in length for same diameter hence passive resistance was mobilized to increase the embedment length of a pile. Mohamedzein et al. [5] found that, the ultimate lateral capacity increases with the increase in slenderness ratio and the pile diameter. It is also observed that, the maximum bending moment (BM) occurs at a depth varying from 0.13 to 0.32L and the bored method of installation gives greater ultimate soil resistance than the pre-installed method for both concrete and steel piles. Sawant and Shukla [4] found that, the pile top lateral deflection and the bending moment (BM) of the pile decreases with an increase in the edge distance from the slope crest. They have been also concluded that, an increase in the ground slope causes the pile deflection and bending moments at any depth of the pile. Mahmoud and Burley [19] observed that, the lateral ratio H/H_{100} and displacement ratio x/B of piles are related in a non-linear fashion. In the analysis of the influence of pile size, the effect of the cross-sectional shape of piles is important. Square piles consistently exhibit greater load capacity than circular piles, although the difference becomes less marked at high displacement ratios. Muthukkumaran [2] investigated that, the horizontal load capacity of the pile, lateral load-lateral displacement response, effect of slopes and embedment length on pile capacity and bending-moment (BM) profile along the pile shaft were studied.

Sundaravadivelu [11] studied the results of laterally loaded pile in soft clay, the iterative procedure was adopted to present a non-linear finite element analysis and the effect of static lateral load on load-deflection behaviour. Kahyaoğlu et al. [9] have analyzed the model of passive piles; the pile spacing gets larger, as the lateral-loads acting on the pile groups are increased. However, for the pile spacing greater than eight times of the diameter spacing's, each pile behave like a single pile without arching effect. The numerical results indicate that the pile spacing increases, as the horizontal-load acting on the soil mass between piles increased. Chae,

Ugai and Wakai [13] carried out numerous numerical studies using a 3D finite element model and prototype tests on laterally loaded short rigid piles and pier foundation located near a 30° slope. The lateral resistance of pile was found to be decreasing with the change in location closer to the crest of the slope. Zhao et al. [12] results revealed that, the pile groups adjacent to surcharge load results in a significant lateral movement of soft soil and considerably applies pressure on the pile groups, when the pressure acting on a row near to the surcharge load is higher than that of the other row due to arching effects of pile group. Georgiadis and Georgiadis [7] carried out 3D finite element analysis to study the behaviour of piles embedded in cohesive soil in sloped ground under the un-drained lateral-loading conditions for a piles of different diameter and lengths were considered. In this analysis, analytical formulations were also derived for the ultimate load per unit length and the initial stiffness of hyperbolic $p–y$ curves. Zhang et al. [15] analyzed laterally loaded pile groups in sand, the maximum bending moments (BM) were developed in leading row piles and minimum in the trailing row piles. The lateral pile responses over vertical piles were 4% in very loose, 14% in loose, 24% in medium dense and 50% in dense sands. Bisaws et al. [3] carried out experimental investigation of free-head model piles under lateral load in homogenous and layered sand, in this experimental study supplemented by numerical study to determine co-efficient of horizontal modulus of sub-grade reaction (η_h). Relative density of sand, slenderness ratio and embedment ratio of pile were varied. The numerical results were found considerably well with the experimental ones for both long and short piles in homogeneous and layered sand media. It is observed that for layered medium density sand, η_h increased as the overlying weaker sand layer thickness decreased. For short piles, η_h increased with increase in sand compactness and slenderness ratio of pile. Whereas in case of long piles, it increased with sand compactness and decreased with the slenderness ratio of pile beyond the slenderness ratio as 40. Rathod et al. [1] have investigated the effect of slope on soil reaction-lateral displacement (p-y) curves for a laterally loaded pile in soft clay. The results show that the pile top displacement and the bending moment (BM) in the pile decrease with an increase in the slope. Also increase in the ground slope causes an increase in pile displacement and bending moments at any depth of the pile.

From the earlier study, it is clear that only a few limited research works have been carried out on piles subjected to lateral load in layered cohesion-less soil, and the behaviour of pile embedded

in multi-layered of cohesion-less soil requires further study. Hence, this paper aims to fill this gap, an experimental investigation is carried out on single pile and pile group embedded in cohesion-less soil under static lateral load. The main objective of the present investigation is to study the lateral response of the piles located in multi-layered cohesion-less soil with different pile configuration and slenderness ratios (L/d 25, 30 and 38) under lateral load, and also to carry out the finite element analysis using Soil-Works 2D and comparing the results with experimental values.

2. Experimental investigation

2.1 Experimental set-up

Here experimental investigation of prototype is reduced to a model scale of 1/15 (1/N) scaled model would require that a prototype pipe pile of 14.60m long by 0.36m circular diameter modelled by stainless steel pipe pile of 0.973m long (overall length) and 24mm external diameter with 2mm wall thickness was used as a model pile (prototype dimension/N). Figure 1 is the layouts of single and pile group of the model, which was modelled in the experimental investigation at 1/15 scale. The Young's modulus ($E_m = 1.617 \times 10^8 kN/m^2$) and the moment of inertia of the model pile (I_m) determined as $4.787 \times 10^{-9} m^4$ and Poisson's ratio (μ) as 0.30. The bending stiffness, $E_m I_m$, of 0.774058kN-m^2. The dimensions of test tank is decided based on the influence zone of soil mass of pile about 10 times the pile diameter in the direction of loading for piles under static lateral load by Poulos [23] and Rao et al. [16]. Hence, the static lateral load tests were conducted in a test tank with a dimension of 1850mm x 1850mm x 1522mm placed on a loading platform. The static lateral load was applied by means of dead weights (slotted type) placed on a hanger connected to a flexible steel wire, passed over a frictionless pulley supported by a loading platform as shown in Figure 2.
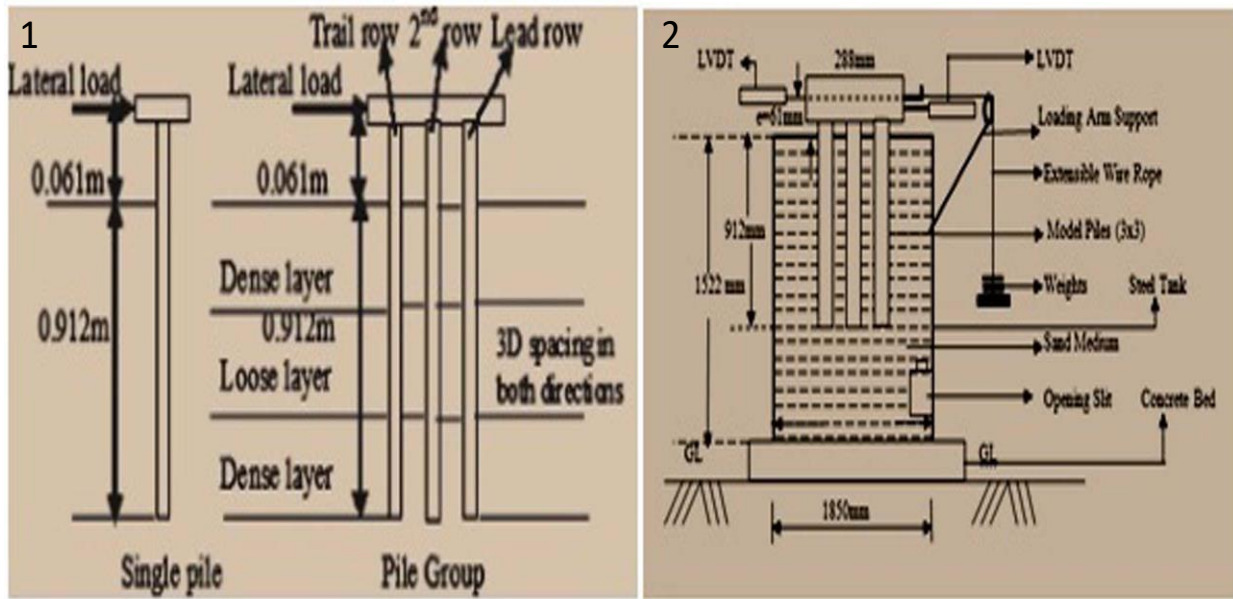
Fig.1. Layouts of single and pile group.   Fig.2. Experimental set-up for lateral load tests.

2.2 Soil used in the experimental studies

In this study a clean dry cohesion-less soil (Indian standard sieve through 1.18mm passing and 75µ retained) is used as the foundation soil. The specific gravity of cohesion-less was found to be 2.67, the minimum and maximum dry unit weights of cohesion-less soil were found to be 16.00 and 19.90kN/m^3 respectively. The particle size distribution was determined using the dry sieving method; the uniformity coefficient (c_u) and coefficient of curvature (c_c) for the cohesion-less soil were 2.41 and 1.20 respectively. A grain size distribution curve of the sand is given in figure 3.
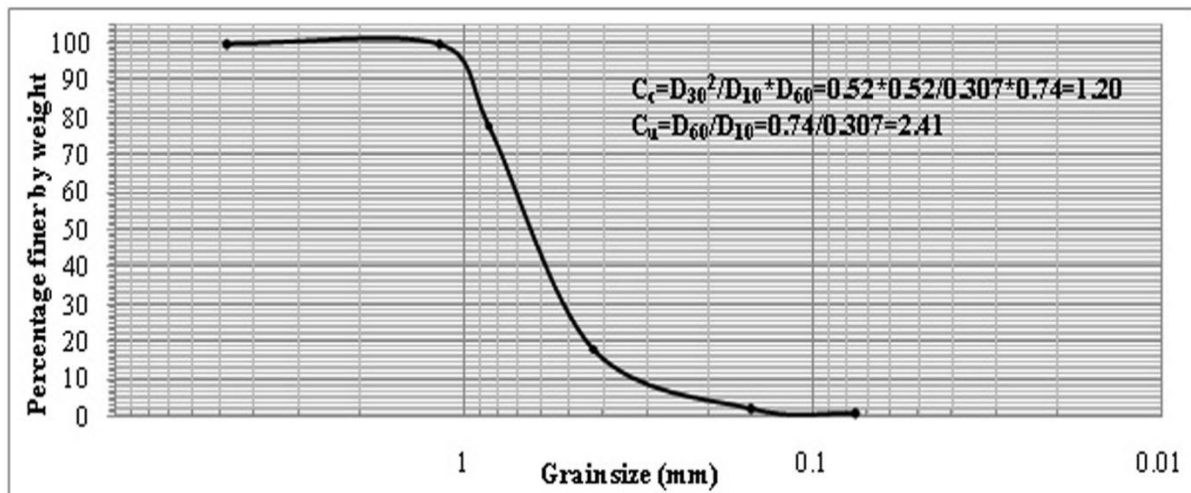
Fig.3. Grain size distribution curve for cohesion-less soil

215

The laboratory model tests were conducted on cohesion-less soil with maximum and minimum void ratios 0.637 and 0.316, for loose cohesion-less soil and dense cohesion-less soil respectively. The relative densities of the cohesion-less soil were 30% and 90% respectively, and the angles of internal friction were 31^0 and 36^0 respectively.

2.3 Experimental procedure

Two different soil medium of loose layer in-between dense layers and dense cohesion-less soil layer were used to carry out the experiment. The two soil mediums were considered as first case and second case respectively in the experiment. Stainless steel pipe piles were used as the model pile in the experimental set up. In first case external lateral load is applied on the model pile embedded in the cohesion-less soil with a depth of 0.456m. The depth of cohesion-less soil was calculated using H/D ratio of 0.50. i.e., H=Dx0.50=0.912x0.50=0.456m. The top and bottom cohesion-less soil layers depth were calculated to be 0.228m each. Using sand raining technique from the height of 600mm from bottom of tank the cohesion-less soil is filled into the tank to get dense state. In second case the depth of the cohesion-less soil was found to be 0.0m which was derived using H/D ratio. The model piles were placed in their positions at the top of the bearing stratum (dense cohesion-less soil layer). The middle layer is filled with the cohesion-less soil from a height of fall 10mm to get loose state; remaining top layer is filled by sand raining technique from a height of 600mm to get dense state. For slenderness (L/d) ratio 25, 30 and 38, the embedment length would be 600, 720 and 912mm respectively from the pile toe. The lateral load is applied at pile head (61mm above the ground surface). For each increment of lateral load, the lateral displacement of pile was measured at pile head using LVDT (Linear varying differential transducer) instrument with display unit. When the lateral displacement of the pile ceases, the next lateral loads increment was applied till the lateral displacement reaches 10.50% of pile diameter (0.105d) and the corresponding load was taken as allowable lateral load capacity of the pile by Rao et al. [16], Chandrasekaran et al. [8].

3. Numerical investigation

3.1 Pile-soil models and parameters

The interactions between the foundation soil and the piles would be the best modeled by a finite element program capable of solving two-dimensional problems. To give some understanding of the complex interactions between foundation soil and piles it was decided to use the computer program Soil works 2D for numerical investigation. The interactions between the soil and the piles can be completely obtained by using 2-dimensional Finite element analysis software. Description of the capabilities of Soil works 2D are presented below.

Soil works 2D 2013(v2.1) is all-in-one 2D Finite element analysis and analytical software for structural and geo-technical engineers. **Soil works 2D** is fully integrated pre/post and solve, complete FEM Software package, CAD based environment, intuitive, automation and robust. This software workflow is as mentioned below;

1. Geometry Modeling, 2. Properties / Meshing / Loads / Boundaries, 3. Analysis and 4. Post-Processing.

The workflow of the Foundation module of Soil works 2D was used as a basis for undertaking p-y analysis is as follows: Step1- define ground material properties; Step 2- define pile material properties; Step3- Input ground layer thickness, assign ground properties and ground water level; Step 4- define foundation type (Pile layout & length); Step 5- specify forces applied to foundation; Step 6- define analysis cases and design options; Step7- execute analysis and step 8, analyze results. The input parameters used in this analysis are presented in Table 1.

Table 1 Pile properties

Sl. No.	Parameters	Notation	Stainless steel pile
1	Material model	----	Linear elastic
2	Element type	----	Beam element
3	Diameter (m)	D	0.024

4	Shape		Pipe
5	Material type		Stainless steel pile
6	Modulus of elasticity (kN/m^2)	E	1.903×10^8
7	Poisson's ratio	µ	0.31
8	Unit weight in kN/m^3	γ	78.50
9	Pile length (m)	L/d=25	0.600
		L/d=30	0.720
		L/d=38	0.912

In an embedded pile consists of beam elements with special interface elements provided such that, the interaction between the beam and the surrounding soil. The beam elements are considered as linear elastic and its behaviors are defined using the elastic stiffness properties. Also the behaviour of interfaces for the modeling of soil-pile interaction is considered with elastic-plastic model. The beam elements are of three-node line elements with six degrees of freedoms per node, three translational degrees of freedoms (u_x, u_y, and u_z) and three rotational degrees of freedoms (φ_x, φ_y, and φ_z). In this present study, the pile is modeled as embedded pile with free connection at its top. The material parameters of the embedded pile distinguish between the parameters of beam, skin resistance and foot resistance. The material properties used in analysis are presented in Table 2.

Table 2 Summarizes the material (ground) properties used in the analyses

Sl. No.	Parameters	Name	Dummy soil	Dense cohesion-less soil	Loose cohesion-less soil	Dense sand
1	Material model	Mode	Mohr-	Mohr-	Mohr-	Mohr-

218

		l	coulomb	coulomb	coulomb	coulomb
2	Material behavior	Type	Drained	Drained	Drained	Drained
3	Unsaturated unit weight(kN/m^3)	γ_{unsat}	0.001	19.90	16.00	19.90
4	Saturated unit weight (kN/m^3)	γ_{sat}	0.001	21.00	18.0	21.00
5	Young's modulus (kN/m^2)	E	0.010	21000	15000	15000
6	Poisson's ratio	μ	0.005	0.30	0.40	0.30
7	Cohesion (kN/m^2)	C	0.1	1	1	1
8	Friction angle (^{0})	Φ	1	36	31	36
Material type		----	Cohesion-less soil (Rees et al.)	Cohesion-less soil (Rees et al.)	Cohesion-less soil (Rees et al.)	Cohesion-less soil (Rees et al.)
9	Horizontal reaction (kN/m^3)	K_h	0.271	16300	7872	16300
10	Strain at 50% Stress		----	----	----	----
11	Unit ultimate skin friction (kN/m^2)	----	6.90×10^{-3}	40	21	40
12	Unit ultimate bearing capacity (kN/m^2)	q_u	6.90×10^{-3}	4000	600	4000

Using the surfaces assigned with material properties, mesh is generated in Soil works 2D software. Figure 5 shows the typical discretization of 2D finite element model of soil-pile-with pile raft structure for nine stainless steel pipe pile group in loose layer in-between dense layers at an eccentricity of 61mm above the ground level for soil model of slenderness ratio (L/d) 38. The program contains p-y curves which can be used for different types of soils. The program also allows the user to input p-y curves developed using the other formulations. The analyses carried out in this study for the piles were discretized into 100 elements in the Soil works 2D program.

219

To explain the laterally loaded single pile behaviour, Soil works 2D uses the soil reaction-lateral displacement (*p-y*) curves as suggested by Reese et al. [24] for the lateral displacement and soil-pile interaction. The soil modulus of the initial linear part *k* is assumed to be increase linearly with embedded depth z by Eq. 1 below:

$$k=n_h z \tag{1}$$

where, n_h= constant of modulus of subgrade reaction. The ultimate soil resistance is mobilized at a lateral displacement of 0.0375times the pile diameter (3b/80) where b is the diameter of model piles.

The model layouts for the single pile and the pile group are shown in Figure 4.
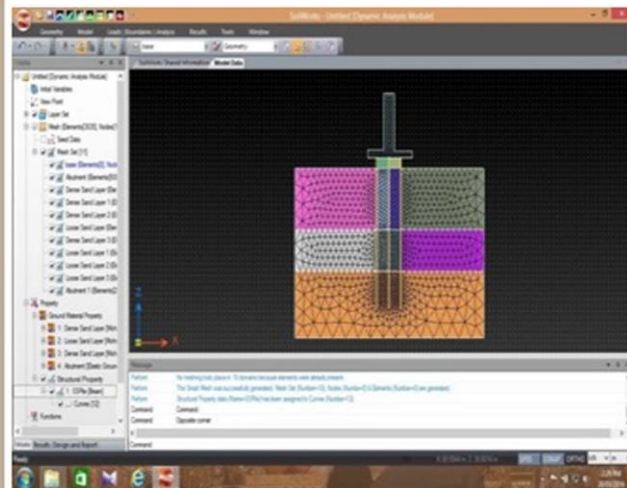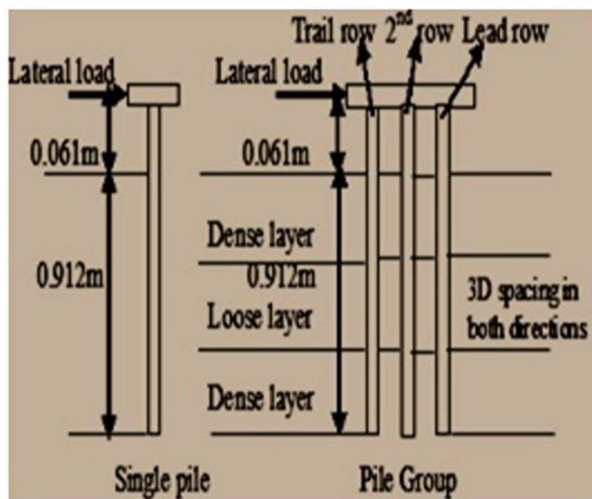
Fig.4. Layouts of single and pile

Fig.5. 2D Finite element model of soil-pile-with pile raft structure for nine pipe pile group in loose layer in-between dense layers

4. Discussion of the experimental and numerical investigation results

The lateral-load behaviour of the stainless steel piles was studied by the lateral load and lateral displacement curves. The curves are drawn for the lateral-load and lateral-displacement pile head. Figure 6 to Figure 8 shows a typical lateral load-lateral displacement curves for slenderness (L/d) ratios as 25, 30 and 38. For a single stainless steel pipe pile (SSP1) and groups of stainless steel pipe piles (SSPn). It is observed that when number of piles increases from single pile to nine piles, the behaviour of pile is almost non-linear. It shows very clearly that at 2.5mm lateral displacement, the ultimate lateral load capacity increases to 0.059kN, 0.13kN,

0.225kN and 0.488kN for single pile, two piles, four piles and nine piles respectively in loose layer in-between dense layers at 3D pile spacing.

Figures 6 to 8 reports the lateral-load and lateral-displacement curves obtained in the lateral load model tests on stainless steel pipe piles. At low lateral displacement, say less than 0.9 to 2.5 mm or 0.0375 to 0.104 of the pile diameter, the pile response is characterized by a rapid increase in lateral resistance, followed by a further increase with a more pronounced pile groups and an approximately nonlinear trend. The stainless steel pipe pile mobilizes a lateral capacity up to 6.451%, 20.325%, 6.22% and 07.037%% higher than the slenderness ratios 25 and 30 for single, two, four and nine pile respectively in loose layer in-between dense layers. In addition, lower slenderness ratios, especially hollow ones, are prone to increased lateral displacement due to shear deformation effects caused by high ratios of elastic to shear modulus. Within the lower slenderness ratios, stainless steel pipe piles exhibit a lateral resistance higher than that of lower slenderness ratios.

Pile response under lateral loading is typically controlled by the soil density, flexural rigidity of pile and soil–pile
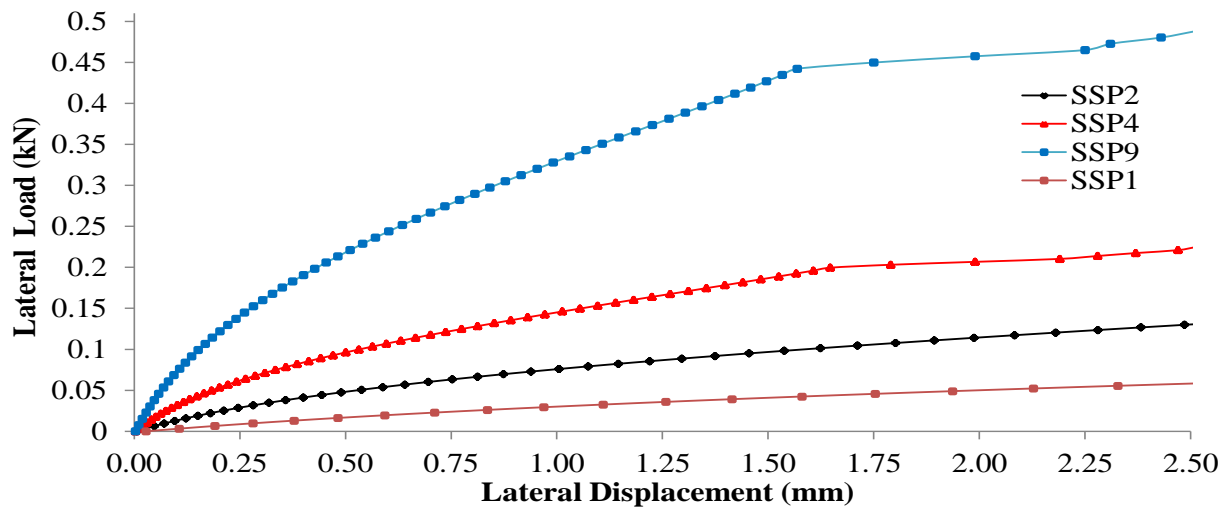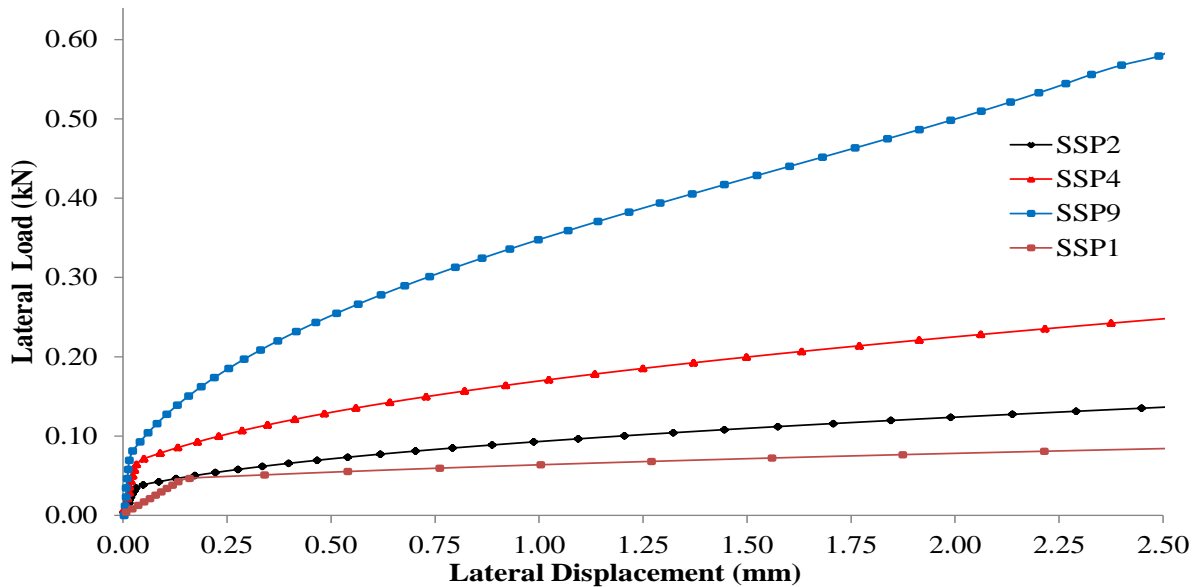

Fig.6. Comparison between single pile and pile group lateral load results of stainless steel pipe piles at 3D pile spacing in loose layer in-between dense cohesion-less soil layers for slenderness ratio as 25.
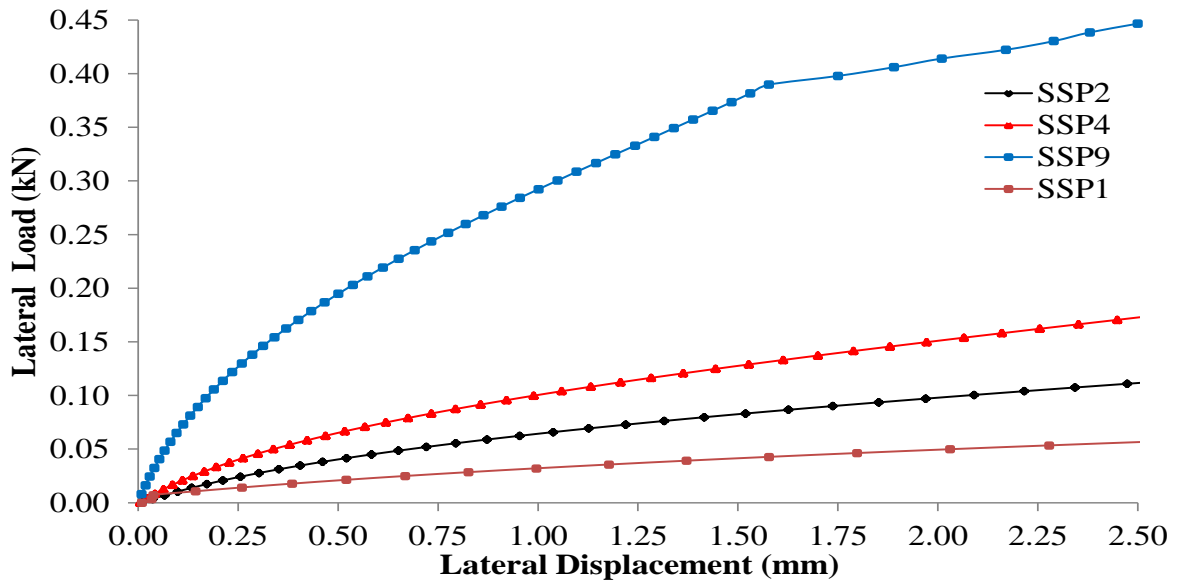
Fig.7. Comparison between single pile and pile group lateral load results of stainless steel pipe piles at 3D pile spacing in loose layer in-between dense cohesion-less soil layer for slenderness ratio as 30.

Fig.8. Comparison between single pile and pile group lateral load results of stainless steel pipe piles at 3D pile spacing in loose layer in-between dense cohesion-less soil layer for slenderness ratio as 38.

interface interaction. In this experiment, lateral displacement response is mainly controlled by the piles flexural stiffness $E_m I_m$ and interface interaction because type of soil layer and type of

222

pile configuration are approximately equal. There are some abnormalities in the initial part of the figures due to change in soil properties and disturbance created when the piles were driven. In general, the lateral loads drop from their initial values, until a lateral displacement level of about 2.5mm a critical, where they remain relatively constant. An initial decrease in resistance with increasing lateral displacement would be estimated for closely spaced piles in a pile group. As the lateral displacements increases, the shear zones began to develop and start to overlap. As the shear zones overlap, "shadowing" effects develop and the soil resistance decreases for the piles in trailing rows.
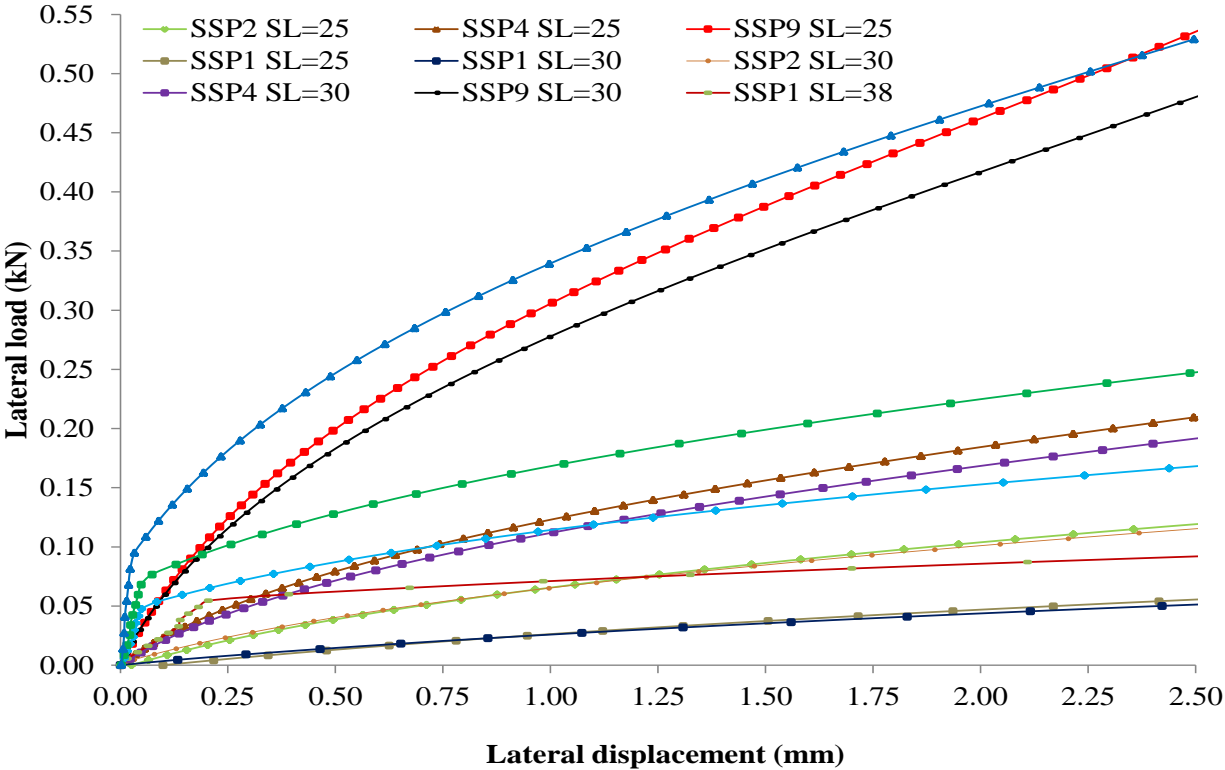
Fig.9. Variations of lateral loads with lateral displacements for different pile lengths of stainless steel pipe piles in loose layer in-between dense cohesion-less soil layers for pile spacing as 3D.
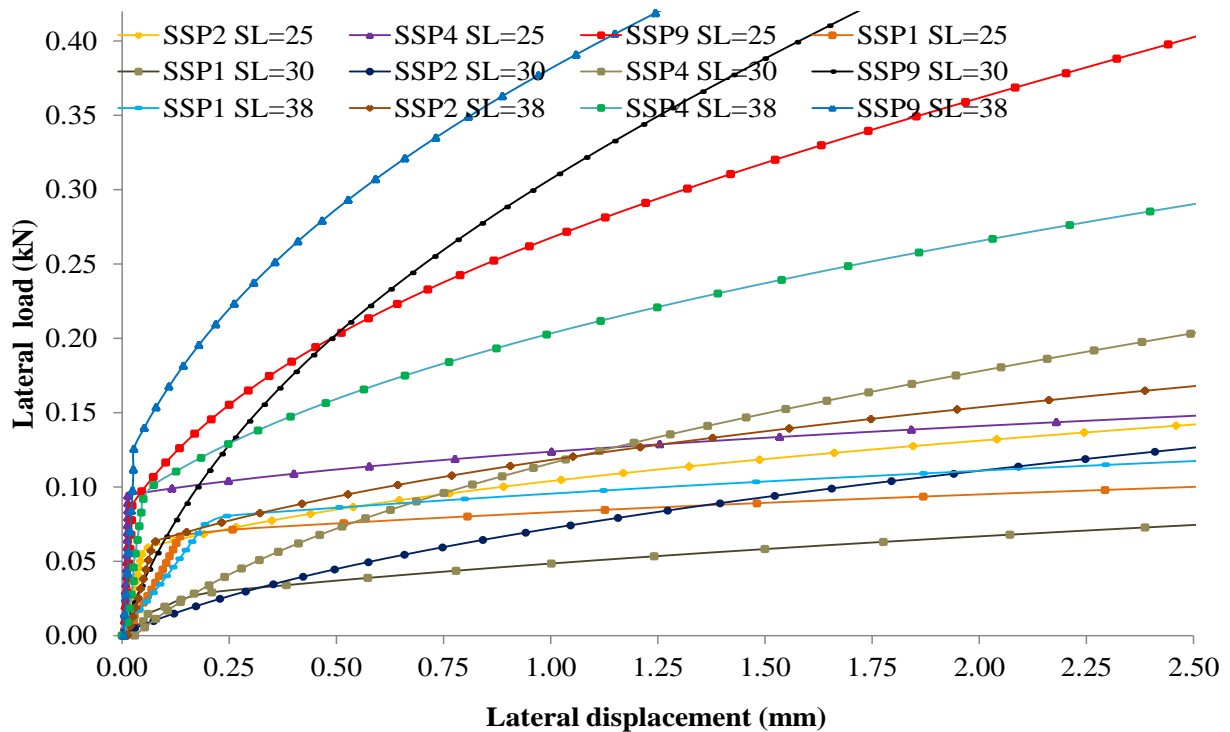
Fig.10. Variations of lateral loads with lateral displacements for different pile lengths of stainless steel pipe piles in dense cohesion-less soil layer for pile spacing as 3D.

From the tests conducted and analysis carried out, the lateral load-lateral displacement curves are obtained. The lateral-load corresponding to a lateral-displacement equal to 10% of a pile diameter is taken as the ultimate lateral capacity of the pile (Broms 1964). Similar consideration is also adopted for pile groups. Figure 9 and figure 10 shows the pile capacity increased with increase in the slenderness ratio of the piles. The increase in capacity is due to increase in the shearing resistance of soil.

The maximum lateral load-lateral displacement curves for the slenderness ratio as 25, 30 and 38 for the three single pile tests are presented in (Figures 9 and 10). For a given lateral displacement, the drop in maximum lateral load from slenderness ratio 25 to 38 is about 17%. Although the difference in the maximum lateral load-lateral displacement curves for the different slenderness ratios is relatively small, these curves are deceptive because they do not show the full lateral load-lateral displacement curve before the maximum lateral load. The complete lateral load-lateral displacement curves as shown in figure 9 to 10. At lateral displacements short of the previous maximum displacement, the load during the SL=25 is significantly below that for the

224

SL=30. The curves for the slenderness ratio as 25 appear to be composed of two segments. The lower part of the curve is relatively linear. The slope of the upper part of the curve increases rapidly and the curve becomes parabolic with a concave upward shape.

This change in slope of the lateral load-lateral displacement curve is readily explained by presence of the gap which developed around the pile. During the SL as 38, the applied lateral load is resisted by both the pile and the near the ground surface. During the continuous loadings, a gap developed between the soil and pile due to the previous lateral loading. For lateral displacement less than the width of that gap, the primary resistance to loading is due to the pile stiffness. This explains the approximate linear relationship between lateral load and lateral displacement when the pile is pushed through the gapped region. As the lateral displacement approached the previously achieved maximum lateral displacement, the lateral load-lateral displacement relationship became non-linear with a concave upward shape. This increase in slope of the upper part of the curve is due to the pile engaging the soil and receiving progressively more lateral soil resistance.

Figures 9 to 10 shows the lateral load lateral displacement response resting on cohesion-less soil, the slope of the lateral load–lateral displacement curves began to increase and diverge as the displacement approached the previous target displacement to which the group was 2.5mm. The curve for the nine pile group shows that the greatest increase in slope. The slope was indicative of the increase in soil resistance as the virgin material was encountered. The slope of the four and two piles remained relatively constant in comparison to that of the nine piles. The group effects decreased the soil resistance for these two rows, therefore, the increase in resistance as the lateral displacement passed the previous level was not as noticeable.

Figures 11 and 12 shows a variation of the lateral-load capacity of pile with slenderness ratios of the different pile materials in loose layer in-between dense layers and dense cohesion-less soil layer, respectively. From these figures, it is concluded that the increase in slenderness ratios increases the lateral-load capacity and decreases in slenderness ratios decreases the pile capacity irrespective stainless steel pipe pile group. It is observed that the lateral-load capacity decreases when slenderness ratios changes from 38 to 30 or 38 to 25 for all the cases irrespective of the dense cohesion-less soil medium to loose layer in-between dense layers.
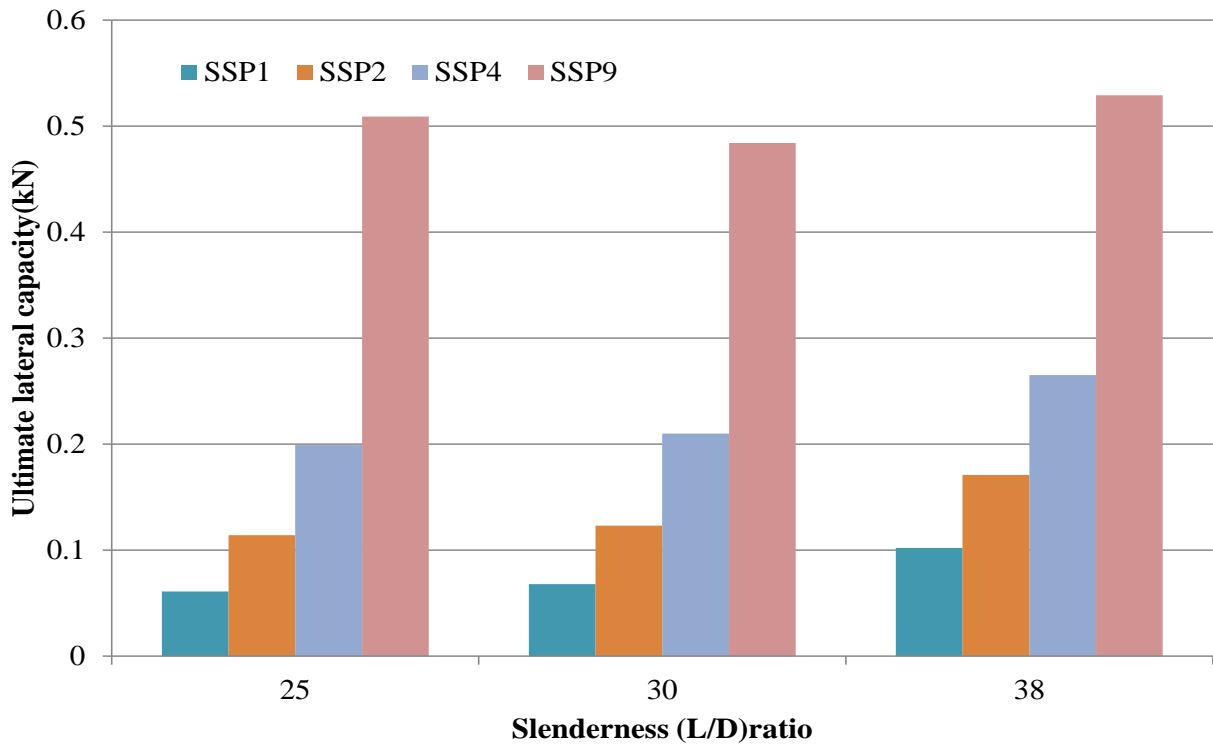
Fig.11. Effect of slenderness ratios on the pile capacity at 3D pile spacing of stainless steel pipe piles in loose layer in-between dense cohesion-less soil layers.
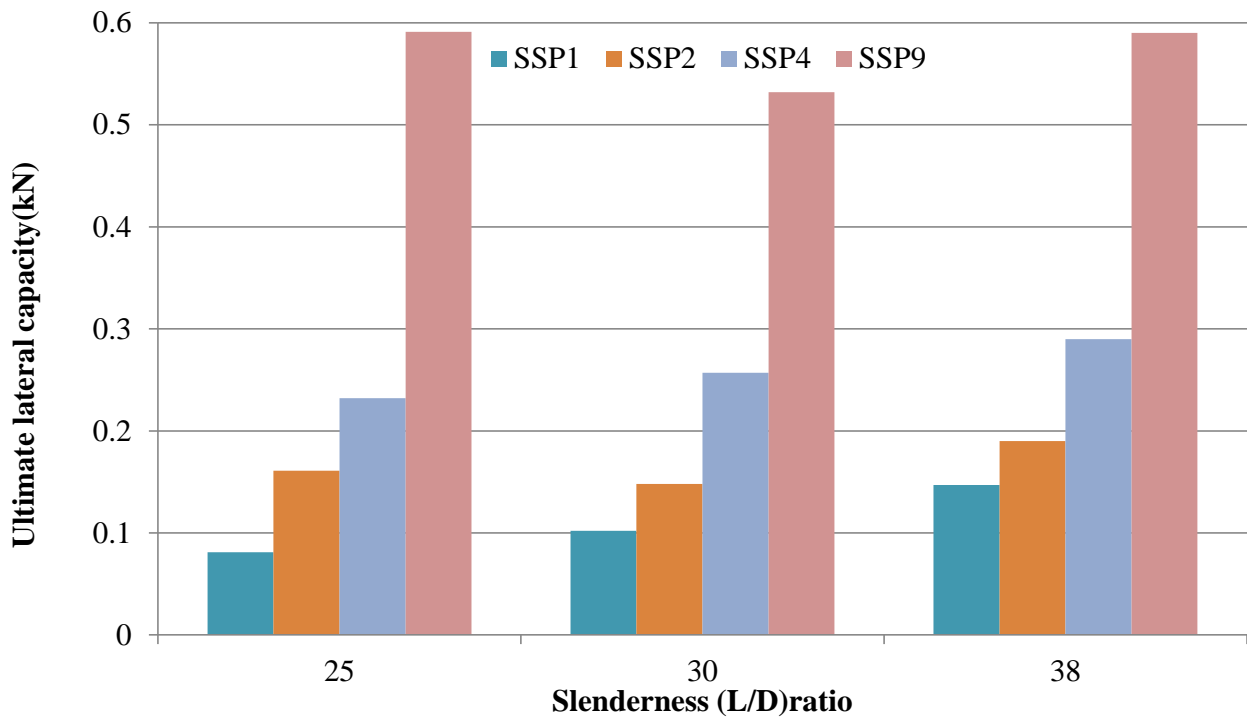
Fig.12. Effect of slenderness ratios on the pile capacity at 3D pile spacing of stainless steel pipe piles in dense cohesion-less soil layer.

When stainless steel pipe pile slenderness ratio=38 to slenderness ratio=30, the percentage reduction in pile capacity is in the range of 7.57-7.85% and when slenderness ratio=38 to slenderness=25, the percentage reduction in pile capacity is quite low, which is in the range of 7.85-7.27% irrespective of all the stainless steel pipe piles.

The lateral load and lateral displacement responses of the piles are measured by experimental investigations and the detailed bending moment, shear force and lateral load versus lateral displacement responses analyzed by Soil Works 2D software are explained below.

4.1 Model pile group

The pile group responses were predicted using Soil Works 2D. The experimental group lateral loads were used in the Soil Works 2D software. Here, the lead row or trail row is defined as per the loading direction. Also, the soil reaction-displacement (p-y) curve and the recommended experimental group lateral loads are at present for monotonic lateral loading only.

227
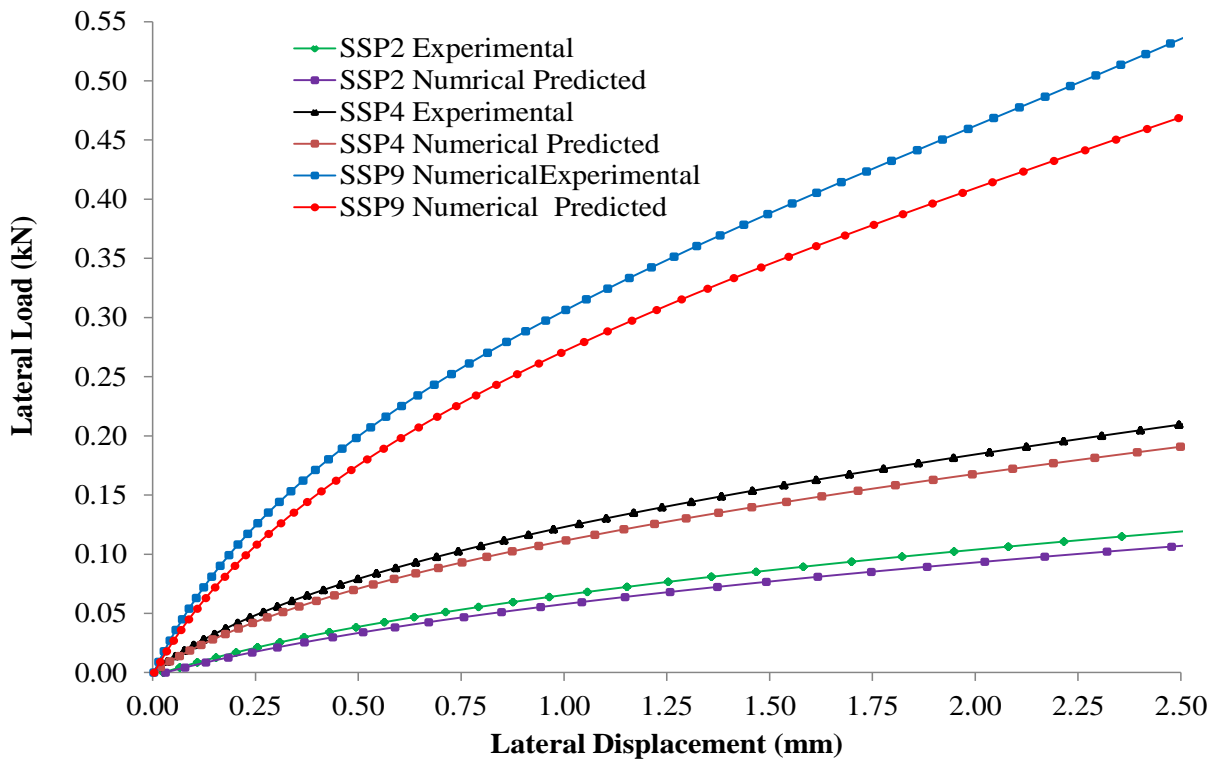
Fig.13. Comparison between the experimental and predicted lateral load results at 3D pile spacing of stainless steel pipe piles in loose layer in-between dense cohesion-less soil layers for SL=25.
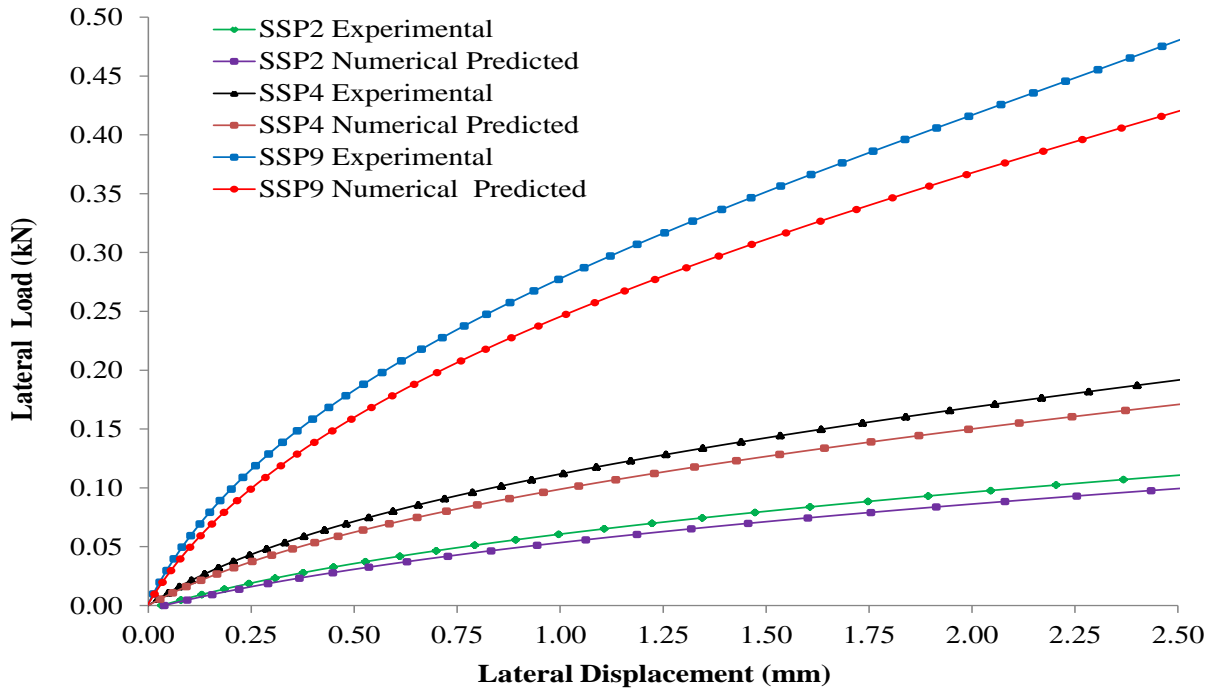

Fig.14. Comparison between the experimental and predicted lateral load results at 3D pile spacing of stainless steel pipe piles in loose layer in-between dense cohesion-less soil layers for SL=30.
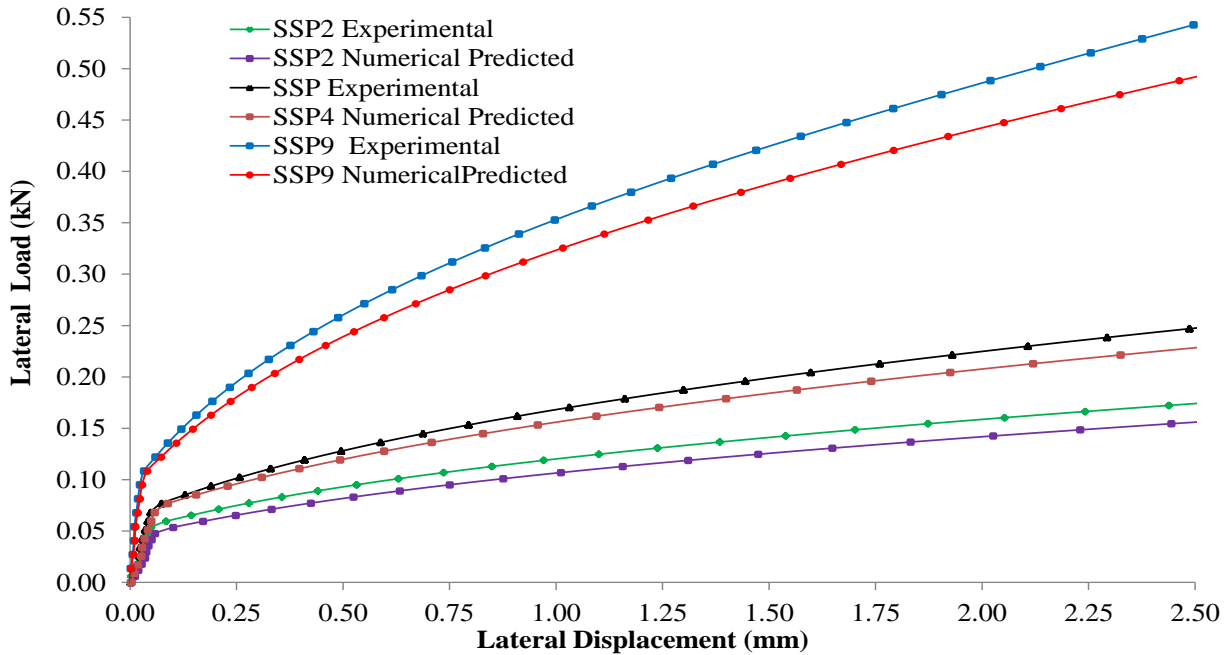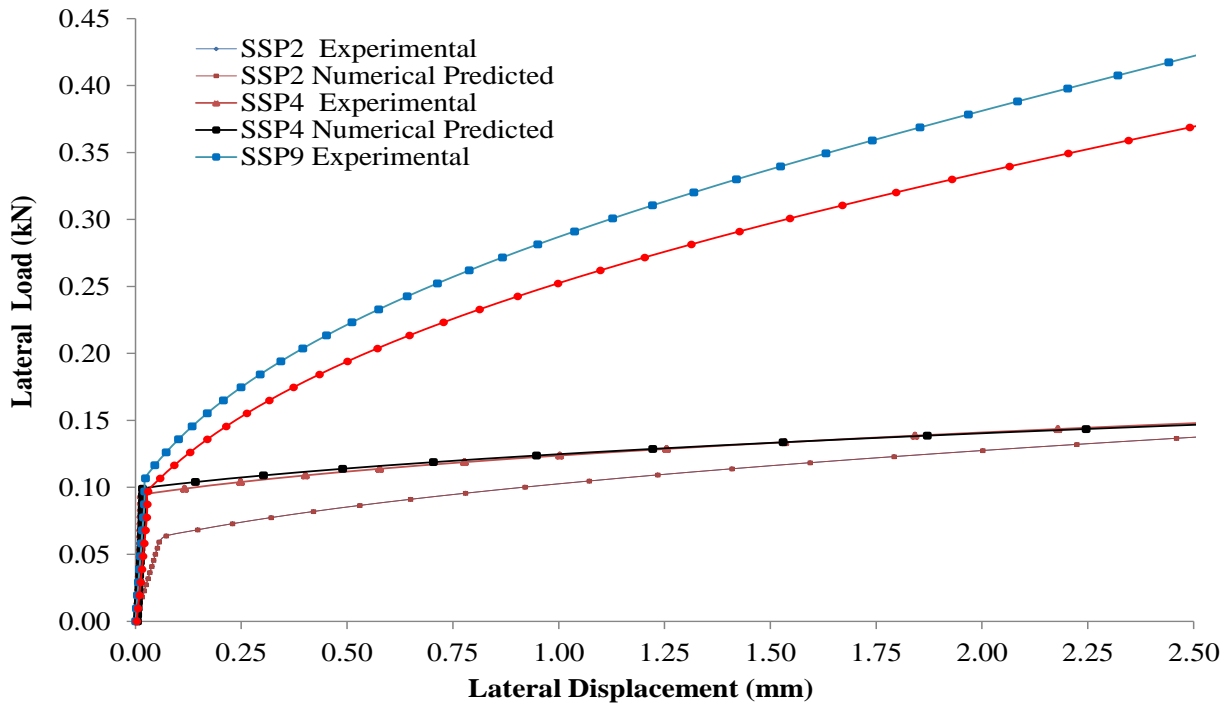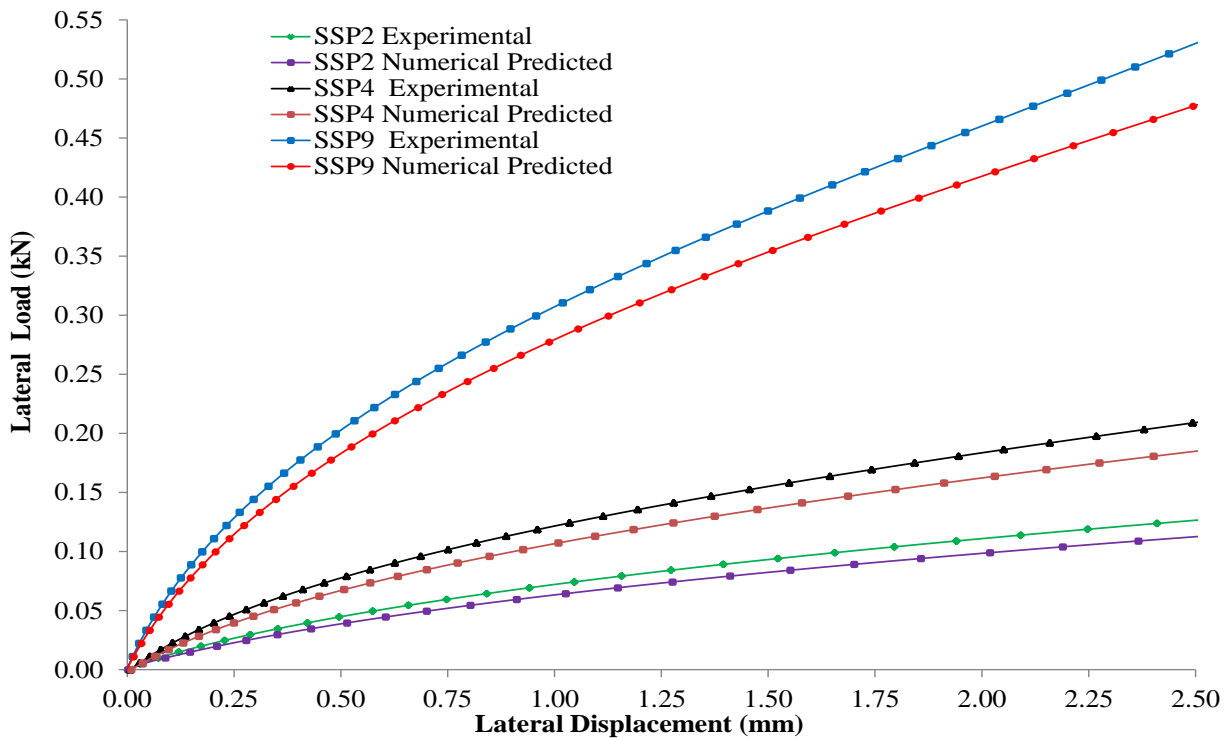
Fig.15. Comparison between the experimental and predicted lateral load results at 3D pile spacing of stainless steel pipe piles in loose layer in-between dense cohesion-less soil layers for SL=38.
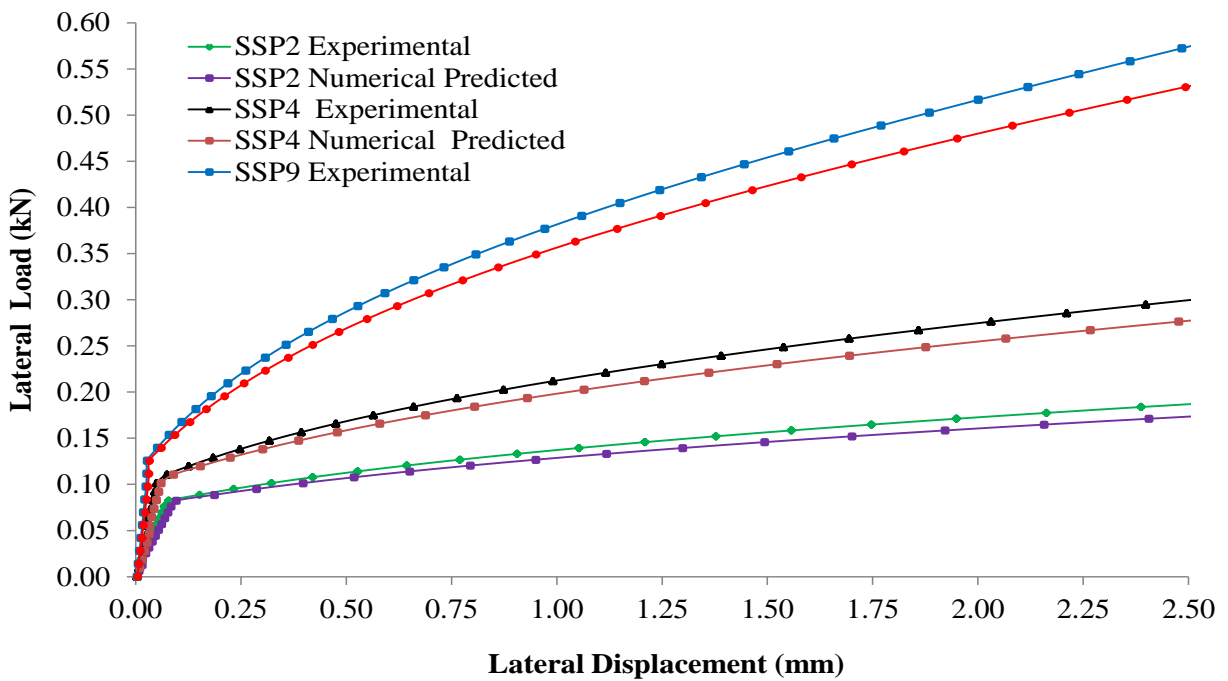

Fig.16. Comparison between the experimental and predicted lateral load results at 3D pile spacing of stainless steel pipe piles in dense cohesion-less soil layer for SL=25.

Fig.17. Comparison between the experimental and predicted lateral load results at 3D pile spacing of stainless steel pipe piles in dense cohesion-less soil layer for SL=30.

Fig.18. Comparison between the experimental and predicted lateral load results at 3D pile spacing of stainless steel pipe piles in dense cohesion-less soil layer for SL=38.

Figures 13 to 18 shows the experimental and predicted lateral load vs. lateral displacement of the pile group in loose layer in-between dense layers and dense cohesion-less soil layer, respectively. It is observed that when two pile group to nine pile group, the behavior of pile is almost like two pile group. It shows very clearly that if pile group decreased from nine piles to two piles, the effect of two pile group is almost small on the lateral load pile capacity. The experimental results are compared with those obtained from finite element analysis (FEA) SoilWorks 2D and found to be in good agreement. Also, it observed that the slenderness ratio increases, the lateral-load capacity increases significantly for both the cases, experimental and finite element analysis (SoilWorks 2D). It is also observed that dense cohesion-less soil layer carries more lateral load compared to a loose layer in-between dense layers for all slenderness ratios. This reduction in pile capacity for a loose layer in-between dense cohesion-less soil layers is because of the reduction in soil density and passive resistance of the soil in front of the pile. The evaluated values are closely match with experimental data quite well. The measured response of the nine pile groups in loose layer in-between dense layers is significantly larger than the predicted response.

Using the Mohr-Coulomb soil model, the pile lateral loads at ground surface were calculated. The calculated lateral loads are shown in (Figs.13 to 18).The predicted values of lateral loads at ground surface show reasonably good agreement with the experimental investigations. These figures also show the predicted values if the flexural stiffness of the pile is modeled as being constant. i.e., independent of the level of applied lateral load. The predicted lateral loads using constant pile flexural stiffness are approximately 7.20% lower than experimental at the pile under large lateral displacement (2.5mm) and the agreement is closer at low lateral loads. This is reasonable since the flexural stiffness of the stainless steel pipe pile is approximately constant up to a lateral loads about 0.10kN. Beyond this lateral loads, the flexural stiffness of this pile decreases almost nonlinearly with increasing applied lateral loads.

For a typical foundation design, pile embedment to pile caps is greater than 2 times pile-diameters to make sure maximum bending moment (BM) transfer between the pile and pile cap.

231

In this study, the piles were embedded 2.54 times pile-diameters into the pile cap. In case of pile head is allowed to rotate, then the maximum bending moment (BM) may occur below its head. It may occur for small fixed-headed group if the pile cap is allowed to rotate
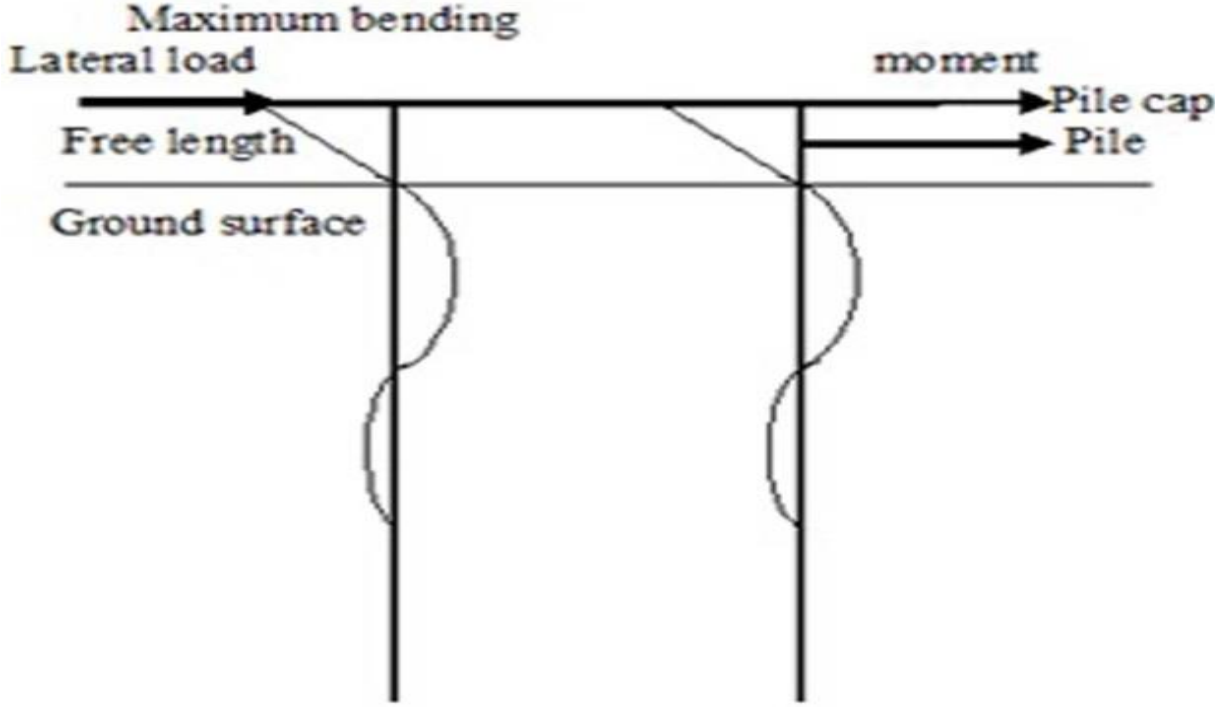
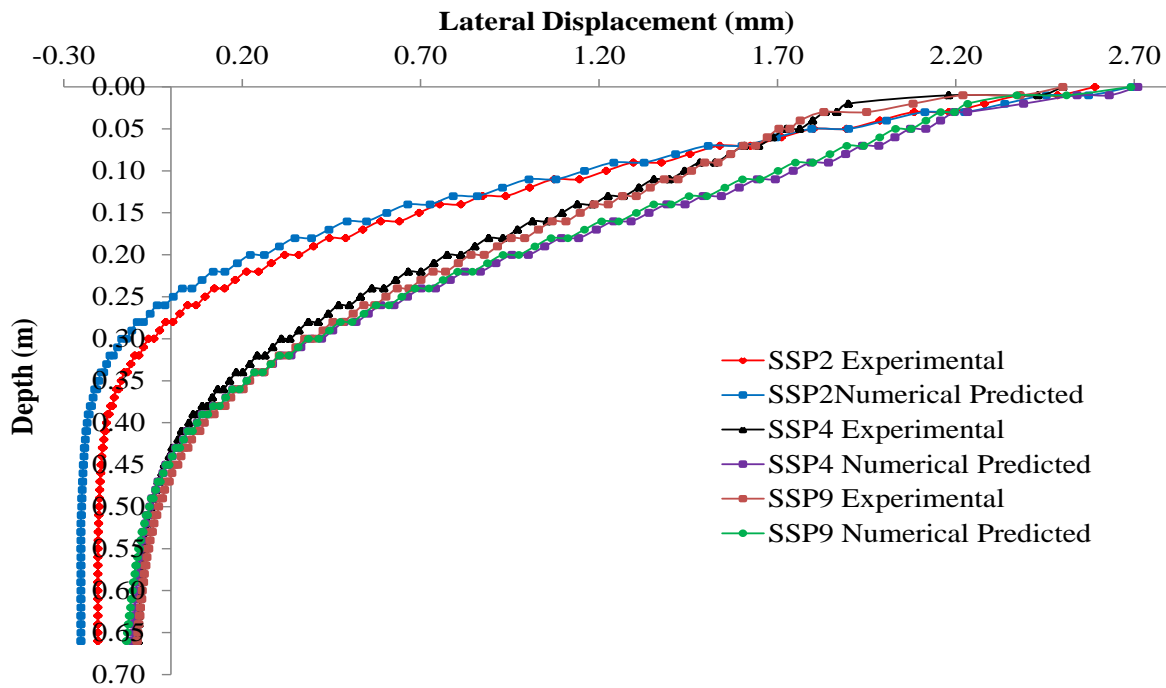Fig.19. Sketch of bending moment distributions free head pile group.

Fig. 20. Lateral displacements along the depth of stainless steel pipe piles in pile group at 3D pile spacing in loose layer in-between dense layers for slenderness ratio as 25.

adequately. Figure 19 showed the typical bending moment (BM) distribution along the pile for this study. The calculated maximum bending moments (BM) for the entire group occurred at the top of each pile or at the pile cap. Hence the maximum bending moments occurring below the ground surface. So that the maximum bending moments and their stresses that control design and consequently has to be modelled accurately.
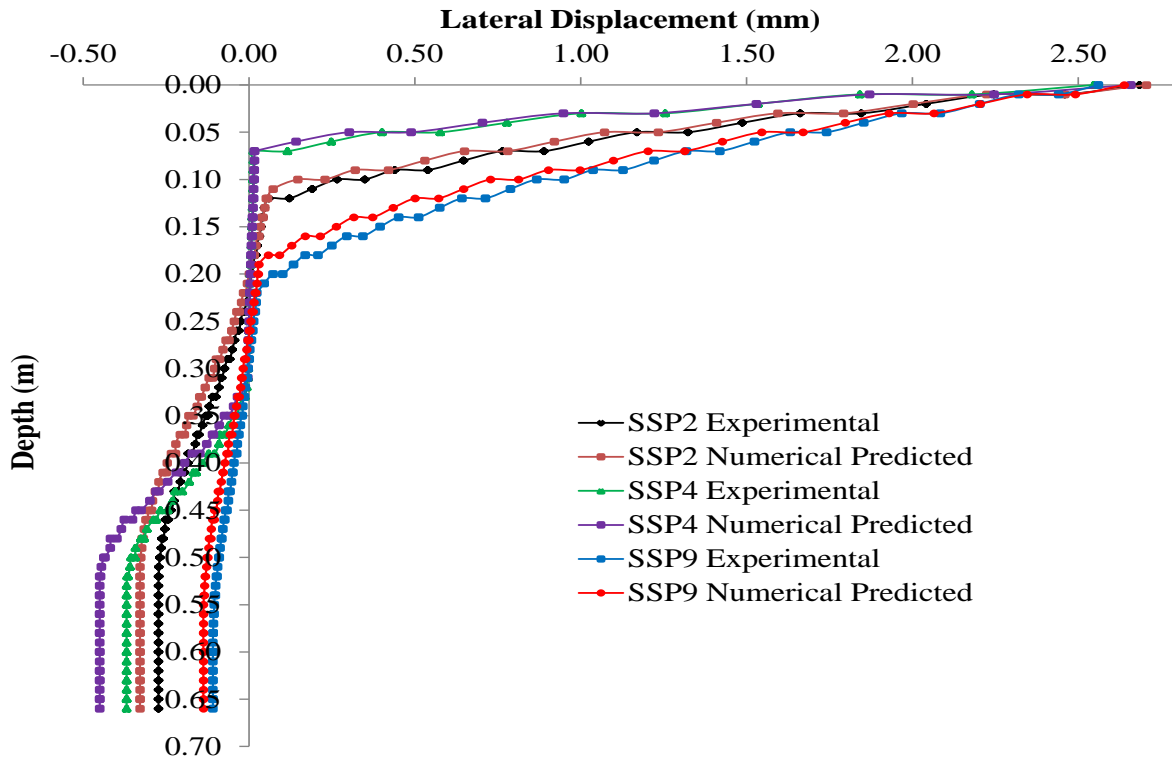
Fig. 21 Lateral displacements along the depth of stainless steel pipe piles in pile group at 3D pile spacing in loose layer in-between dense layers for slenderness ratio as 30.
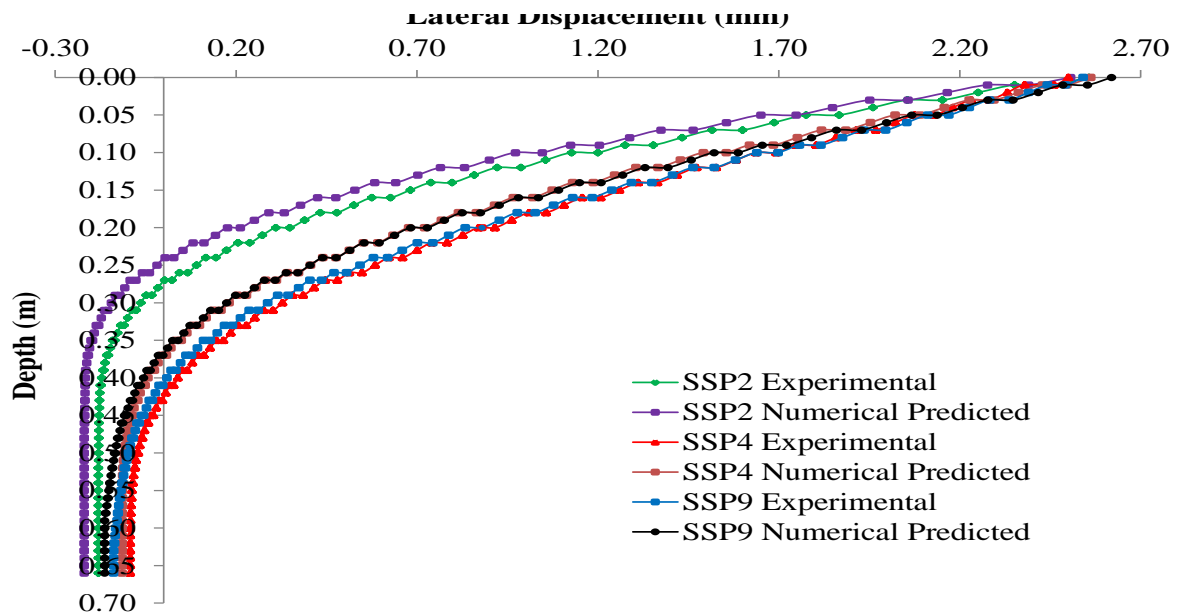
Fig. 22 Lateral displacements along the depth of stainless steel pipe piles in pile group at 3D pile spacing in loose layer in-between dense layers for slenderness ratio as 38.

As the pile cap deflects under lateral load, the piles support it also deflects, as shown in (Figs.19 to 24). The results of the finite element analysis (FEA) show that the soil around the piles moves significantly as the lateral load is applied to the pile cap. The moving soil does not provide as great resistance to movements of the relative movement of the pile with respect to the soil. If the soil around the piles moved the same amount as the piles, the soil would provide no resistance to pile lateral displacement. The piles would deflect as if they were surrounded by air.
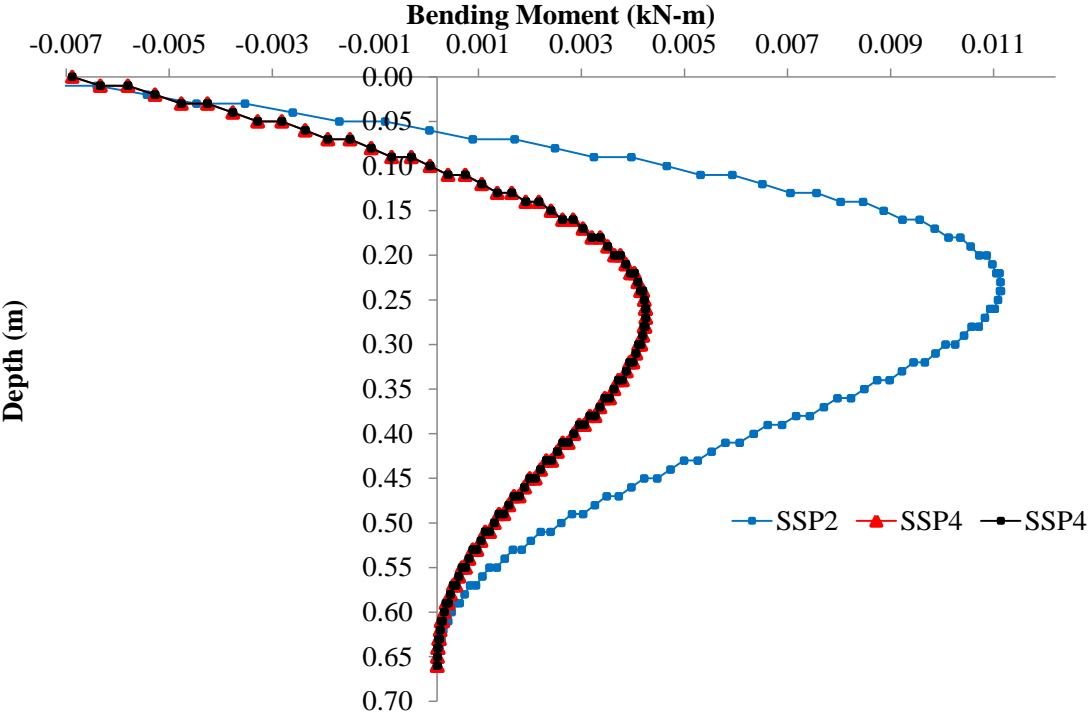

Fig.23. Predicted different pile group bending moments at 3D pile spacing of stainless steel pipe piles in loose layer in- between dense layers for slenderness ratio=25.
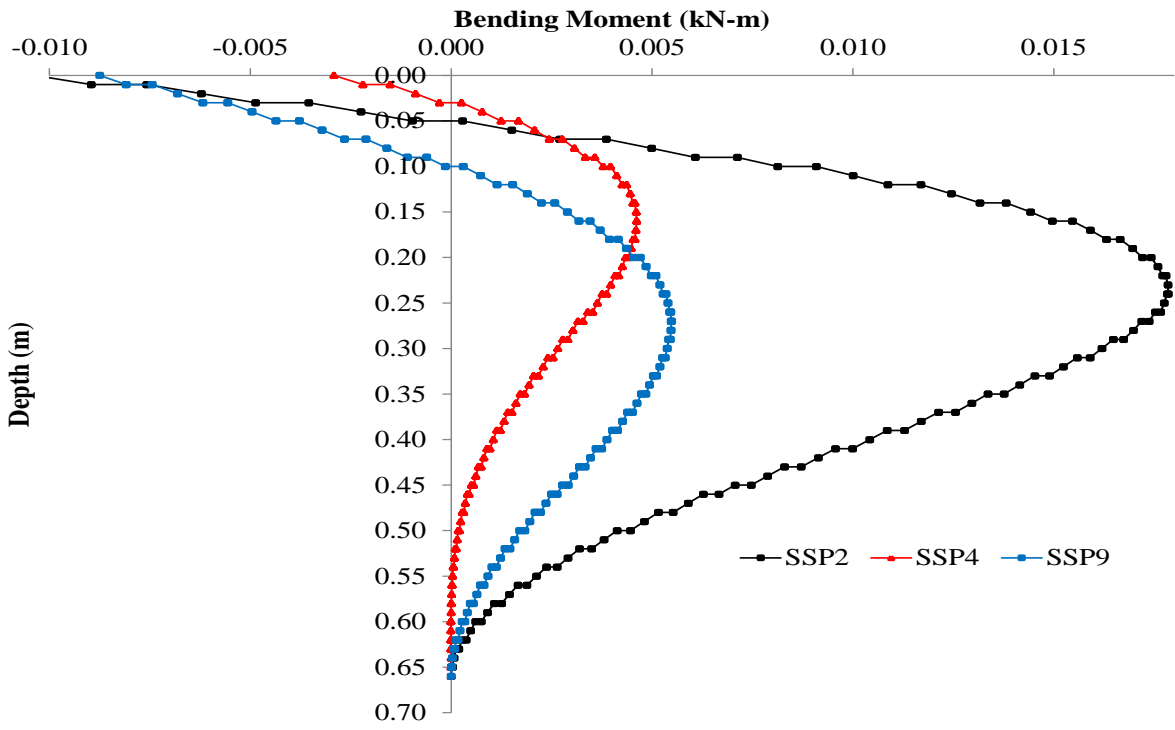
Fig.24. Predicted different pile group bending moments at 3D pile spacing of stainless steel pipe piles in loose layer in- between dense layers for slenderness ratio=30.
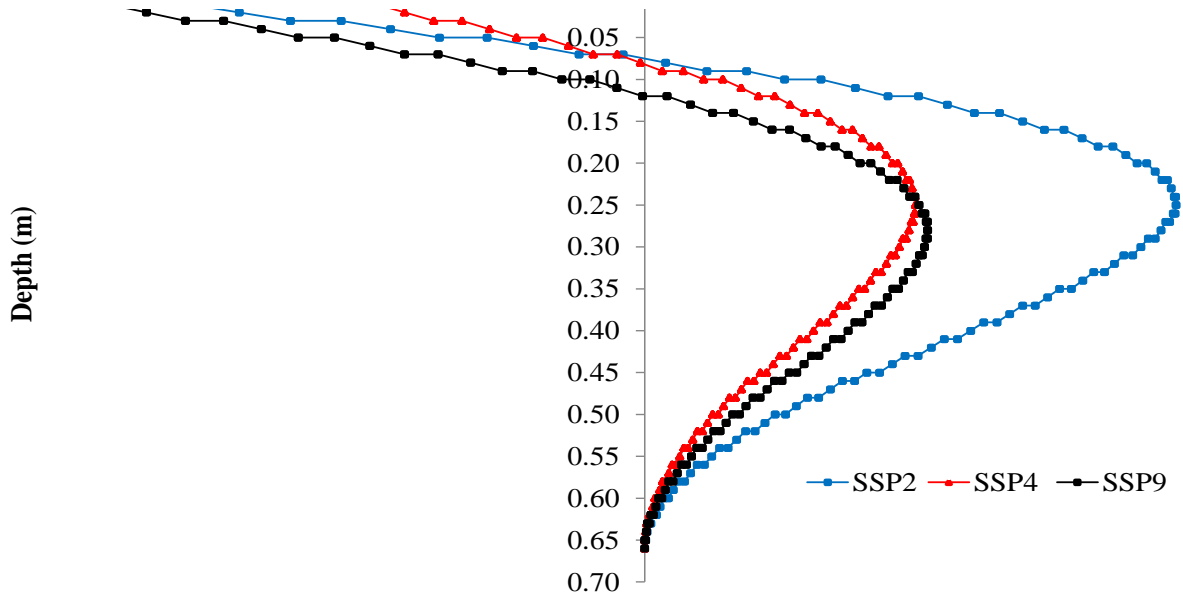

Fig.25. Predicted different pile group bending moments at 3D pile spacing of stainless steel pipepipe piles in loose layer
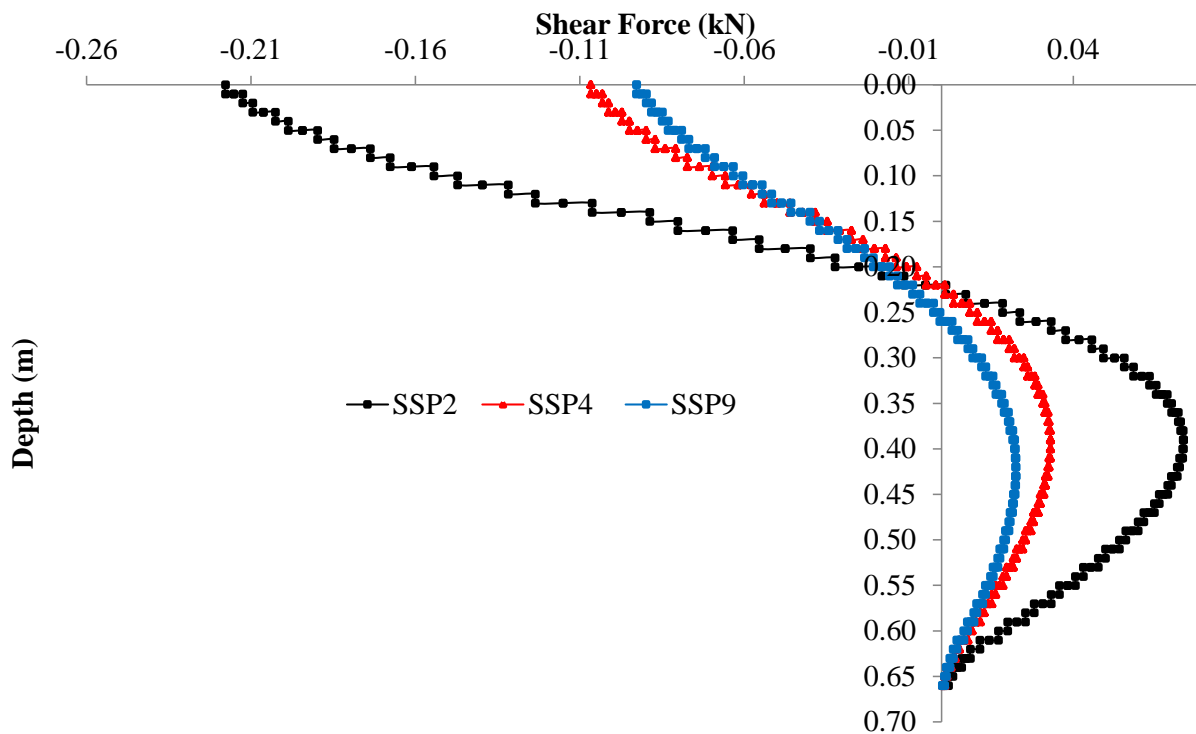
236

Fig.26. Predicted different pile group shear force results at 3D pile spacing of stainless steel pipe piles in loose layer in-between dense layers for slenderness ratio as 25.

Figure 23 to 25 shows the bending moments along the piles for the different pile group of slenderness ratios 25 to 38 in the loose layer in-between dense cohesion-less soil layers medium. The maximum bending moments (BM) of pile group as shown in figure 23 to 25. Because of the number of piles, the individual pile group (two, four, and nine piles) moments differ significantly, but within a four pile and nine pile group, the difference is negligible. Note that the four piles to nine pile groups develop the same bending moment, because they have the same square pile configuration in both the direction. Also, the maximum moments below the ground elevation are only 8.34% of their pile top values.

At the larger lateral displacement the maximum bending moment that occurred in the two piles is relatively consistent in depth and magnitude with those of the four and nine pile group. However, the two piles bending moment drops off relatively quickly with depth while the pile group bending moments remain relatively high. This difference in moments, due to the group effects, suggests that the moments for which a pile in a group must be designed may be significantly higher at depth than would be expected based on the two piles experimental results.
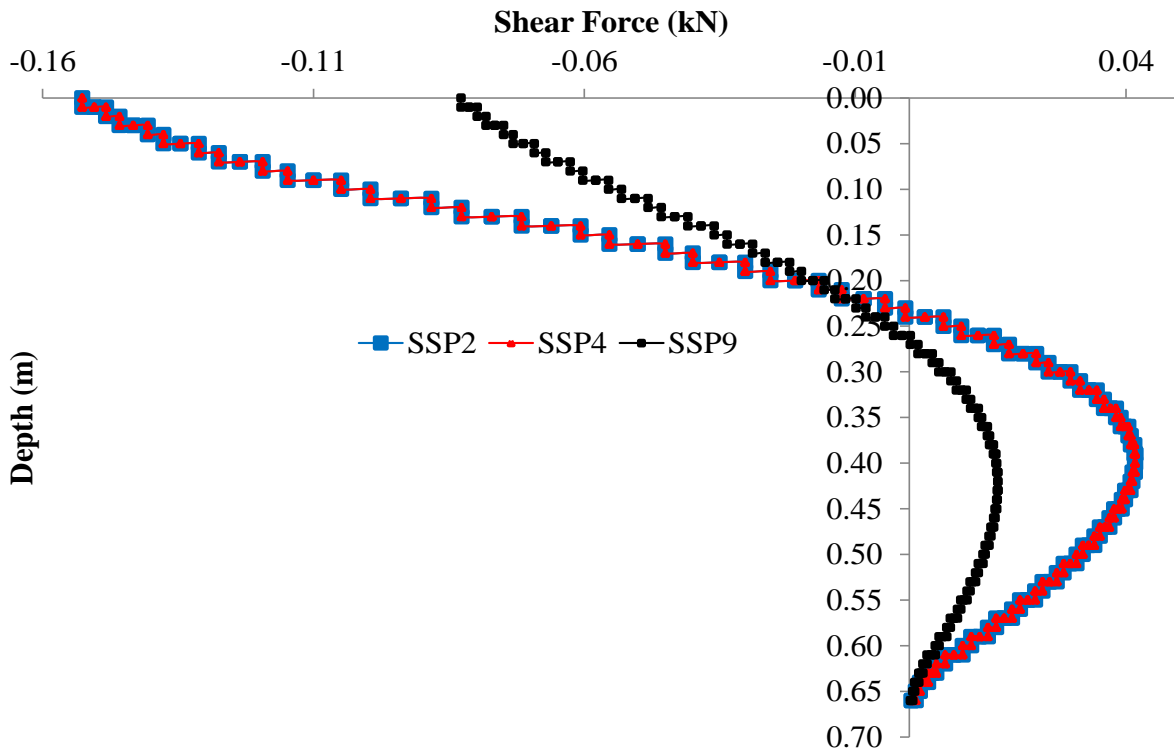
237

Fig.27.Predicted different pile group shear force results at 3D pile spacing of stainless steel pipe piles in loose layer in-between dense layers for slenderness ratio as 30.
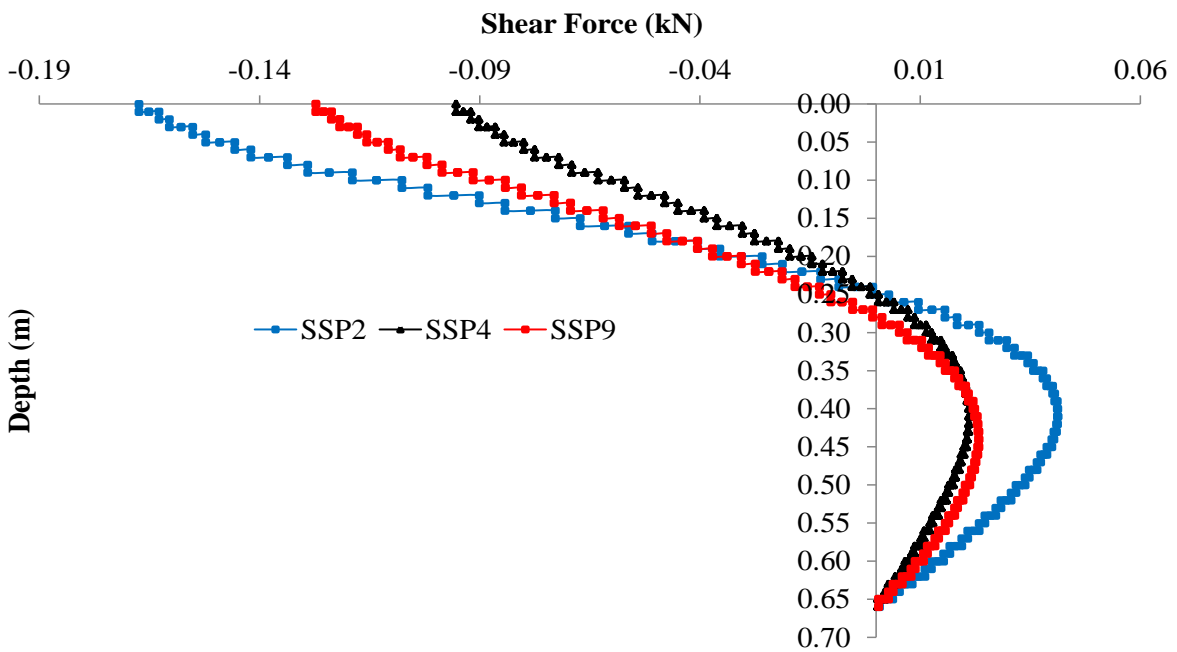

Fig.28.Predicted different pile group shear force results at 3D pile spacing of stainless steel pipe piles in loose layer in-between dense layers for slenderness ratio as 38.

.

Figure 26, 27 and 28 shows these shear force in each slenderness ratio of the different pile group in loose layer in-between dense cohesion-less soil medium. From the figures, it is observed that the maximum shear force increases with decrease in the pile groups (nine pile group to two pile group). Also, for the same length of pile (say 720mm), the shear force is more for loose layer in-between dense layers. This is because of the decrease in the resistance at the top portion of the soil mass as there is a reduction in the soil mass in the loose layer in-between dense layers. Here it is observed that, the depth at which the maximum shear force occurs at depth fixity, decreases with increase

in the flexural rigidity (EI) of the pile and the soil because of the increase in the embedded length of the pile. Since the shear force profile, it observed that, the depth of fixity occurs almost at a depth of 15.41D, 15.83D and 16.25D for stainless steel model pipe piles in loose layer in-between dense layers below the soil surface of slenderness ratios, 25, 30 and 38 respectively. Here this is also observed that, there is little change in depth of fixity because of the variation in soil layer.
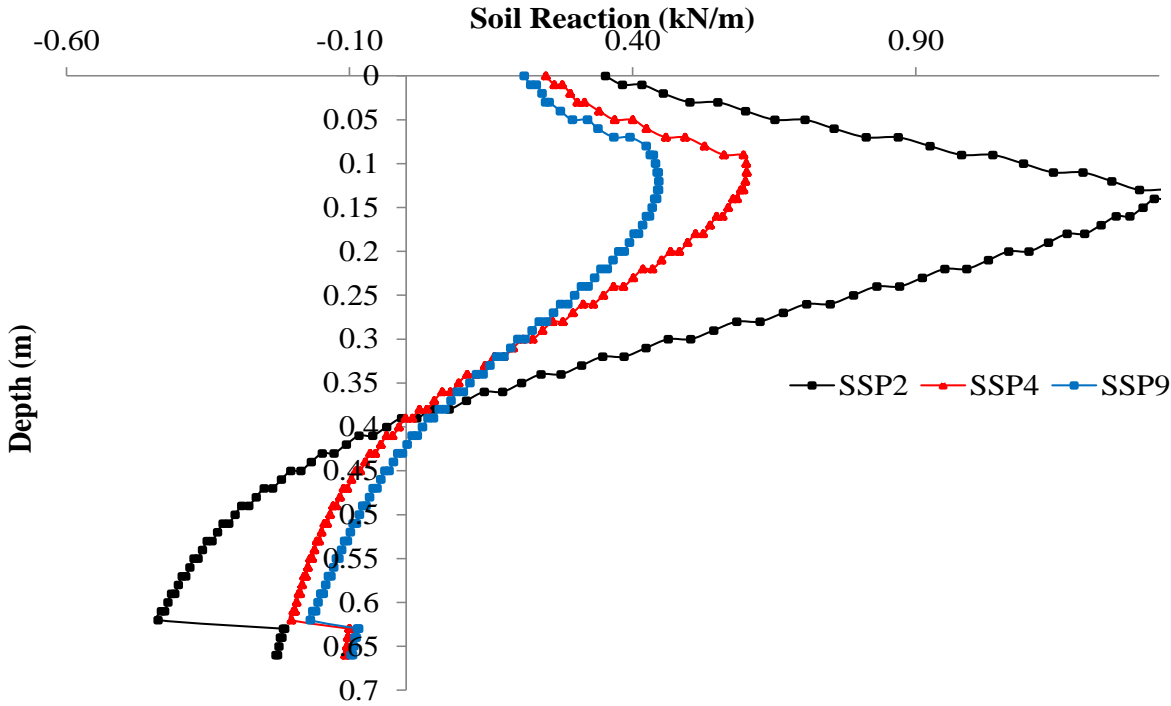

Fig.29. Predicted different pile group soil reaction results at 3D pile spacing of stainless steel pipe piles in loose layer in-between dense layers for slenderness ratio as 25.
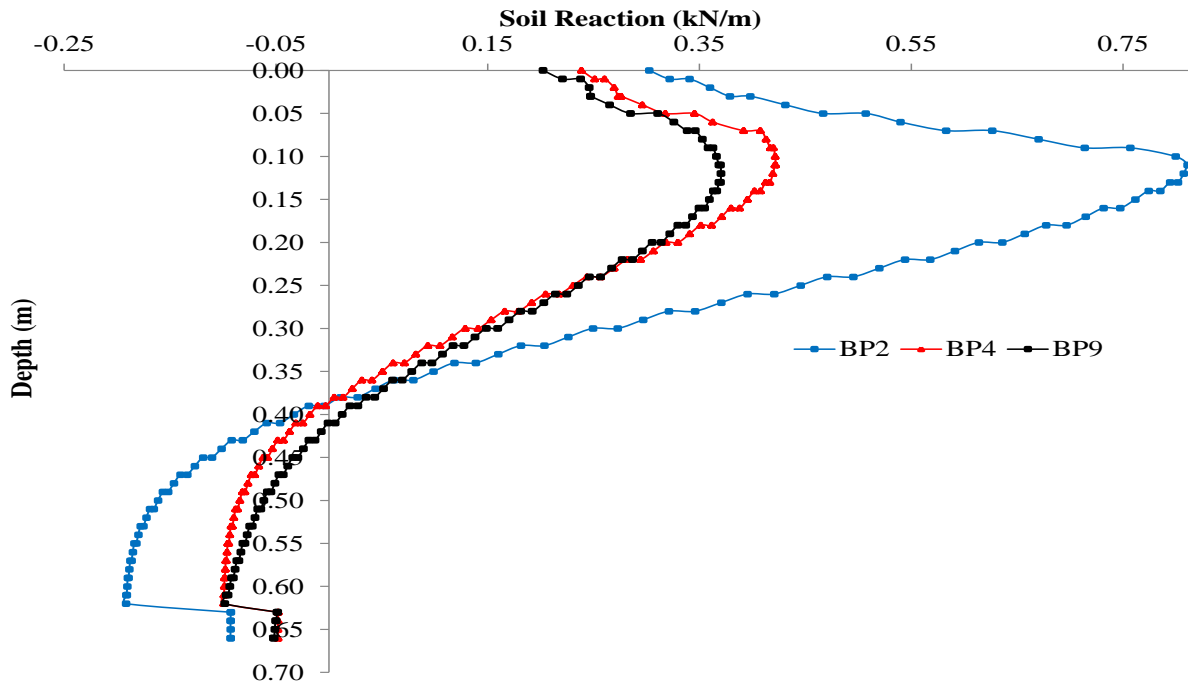
9

Fig.30. Predicted different pile group soil reaction results at 3D pile spacing of stainless steel pipe piles in loose layer in-between dense layers for slenderness ratio as 30.

pile spacing in loose layer in-between dense layers. From the soil reaction profile, here it clearly

seen that, the depth of fixity occurs almost at a depth 4.60D, 5.41D and 5.42D for stainless steel model pipe piles in loose layer in-between dense layers below the soil surface for slenderness ratios, 25, 30 and 38, respectively. Hence, there is little change in depth of fixity because of the variation in soil layer.

5. Conclusions

a. The lateral load experimental test on the bamboo pipe piles showed similar behaviour to that from experimental study and numerical study. The maximum bending moment increases with decrease in the pile groups

b. The soil around the piles moves along the movement of the pile cap. The relative movement between the pile and soil is therefore reduced, resulting in relatively low shear forces at the top of the pile.

c. The increase in lateral load is due to different pile configurations and soil density.

240

d. The experimental lateral loads are found to be dependent on different soil density and pile group configuration.

e. The load carrying capacity of nine piles placed in a group has 5 to 8 times greater load carrying capacity of single pile in loose layer in-between dense layers. The stainless steel pipe piles carry a load of 0.508kN at density 16.00kN/m^3.

f. The ultimate lateral load is considerably reduced when the soil layer changes from loose layer in-between dense layers to dense sand layer. The dense sand layer carries more lateral loads compared to loose layer in-between dense layers for all slenderness ratios.

g. It is found that the lateral load-lateral displacement behaviour is still non-linear with the presence of lateral load and the load carried by 3D pile spacing in loose layer in-between dense soil layers.

h. The behaviour of pile group under lateral loads not only depends on the lateral load and number of piles in a group, but also depends on the soil layer condition and flexural rigidity of pile material.

i. The load carrying capacity of nine piles placed in a group is about 13% greater than that of the single pile in loose layer in-between dense layers.

j. Pile group displacement in relatively loose layer in-between dense layers, is larger than the lateral displacements happens in pile group in dense sand layer as expected.

k. The bending moment, shear force and soil reactions are along the length of pile with same length and different pile diameter, a close matching between the three results were obtained.

References

[1]   D. Rathod, K. Muthukkumaran, T.G. Sitharam, Effect of slope on p-y curves for laterally loaded piles in

soft clay, *J. Geotech. Geologi. Eng.* 2017,1-16.

[2]   K. Muthukkumaran, Effect of slope and loading direction on laterally loaded piles in cohesion-less soil, *Int. Journal of Geotech.Eng.*14 Issue 1, 2014, 1-7.

[3]   S.K. Bisaws, S. Mukherjee, S. Chakrabarti, M. De, Experimental investigation of free head model piles under lateral load in homogenous and layered sand, *Int. J. Geotech. Eng. 1939787914Y-0000000078* (Advance Articles), 2014.

[4]   V.A. Sawant, S.K. Shukla, Effect of edge distance from the slope crest on the response of a laterally loaded pile in slopping ground, *Geotech. Eng.* 32 Issue 1, 2013, 197-204.

[5]   Y.E.A. Mohamedzein, F.A.E. Nour Eldaim, A.B. Abdelwahab, Laboratory model tests on laterally loaded piles in plastic clay, *Int. Journal of Geotech. Eng.* 7 Issue 3, 2013, 241-250.

[6]   K. Georgiadis, M. Georgiadis, Development of p-y curves for undrained response of piles near slopes, *Comp. Geotech*. 40, 2012, 53–61.

[7]   K.Georgiadis, M.Georgiadis, Undrained lateral pile response in sloping ground, *J. Geotech. Geoenviron. Eng.* 136 Issue 11, 2010, 1489–1500.

[8]   S.S. Chandrasekaran, A. Boominathan, G.R. Dodagoudar, Group interaction effects on laterally loaded piles in clay, *Journal of Geotech. and Geoen. Eng.*130 Issue 4, 2010, 573-582.

[9]   M.R.Kahyaoğlu, G. Imancli, A.U. Öztürk, A.S. Kayalar, Computational 3D finite element analyses of model passive piles, *Computational Materials Science 46*, 2009,193-202.

[10]   U.Salini, M.S. Girish, *Lateral load capacity of model piles on cohesion-less soil*, *EJGE,* Vol. 14, 2009, 1-1.

[11]   R. Sundaravadivelu, K. Muthukkumaran, S. Gandhi, Effect of slope on p-y curves due to surcharge load, *Soils Found*.,48 Issue 3, 2008, 353–361.

[12]   M. Zhao, D. Liu, L. Zhang, C. Jiang, *3D finite element analysis on pile-soil interaction of passive pile group, J.Cent South University Technological,* Vol.15, 2008, 75−80.

[13]   K.S. Chae, K.Ugai, A. Wakai, Lateral resistance of short single piles and pile groups located near slopes, *Int. J. Geomech.*4 Issue 2, 2004, 493–103.

[14]   K. Byung-Tak, K. Young-Su, Back analysis for prediction and behaviour of laterally loaded single piles in sand, A*SCE journal of civil engineering*, 3 Issue 3, September 1999, 273-288.

[15]   L, Zhang, M.C. McVay, P.Lai, Numerical analysis of laterally loaded 3x3 to 7x3 pile groups in sands, *J.Geotech. Geoenviron. Eng.* 125 Issue 11, 1999, 1-16.

[16]   S. Narasimha Rao, V.G.S.T. Ramakrishna , M.B.Rao, Influence of rigidity on laterally loaded pile groups in marine clay, *Journal of Geotech. Eng.* 124 Issue 6, 1998, 542-549.

[17] M.C. McVay, T. Shang, R. Casper, Centrifuge testing of fixed-head laterally loaded battered and plumb pile groups in sand, *Geotechnical Testing Journal* 19 Issue 1, 1996b, 41-50.

[18] S. Prakash, Sanjeevkumar, Nonlinear lateral pile deflection prediction in sand, *Journal of Geotech. Eng. ASCE,* 122 Issue 2, 1996, 130-138.

[19] M. Mahmoud, E.Burley, Lateral load capacity of single piles in sand, *Procceding, Institution of Civil Engineers, Geotechnical Engineering*, July 1994, 107,155-162.

[20] J.M. Kulicki, D.R.Mertz, I.M.Priedland. LRFD bridge design code, Report of NCHRP, Transportation Research Board, National research Council, Washington, D.C; 1991, p.12-33.

[21] D.A.Brown, Morrison C, Reese L.C, Lateral load behavior of a pile group in sand, *Journal of Geotech. Eng. ASCE* 112 Issue11, 1988, 1261-1276.

[22] H.G. Poulos, Behaviour of laterally loaded piles. II: pile groups, *Jl. of Soil Mech. and Found. Engg. Div., ASCE,* 97 Issue 5, 1980, 733-751.

[23] G.G. Meyerhoff, Bearing capacity and settlement of pile foundations, *Journal of Geotech. Eng.ng, ASCE*, 102 Issue 3, 1976, 195-228.

[24] Reese LC, Cox WR, Kapoo FD. Analysis of laterally loaded piles in sand. Proceeding 6th Annual Offsore Technology Conference, Houston; paper OTC 2080, 1974, p.473-483.

[25] J.A.Focht, K.J. Koch. Rational analysis of the lateral performance of offshore pile groups. Proceeding of 5th Offshore Technol. Conference, Richardson, Taxas; 1973, p.701-708.

[26] Tomlinson's M.J. Some effects of pile driving on skin friction. Proceeding of Conference on Behaviour of Piles, Institution of Civil Engineers, London, 1971, p.107-114.

[27] M.T. Davisson. Lateral load capacity of piles. Transportation Research Board, National Hghway Research Council, Washington, D.C, 333; 1970, p.104-112.

[28] Deendayal Rathod, D. Nigitha and K.T. Krishnanunni: Experimental investigation on the behavior of monopile under asymmetric two-way cyclic lateral loads, *International Journal of Geomechanics, ASCE*, Vol. 21(3) (2021):06021001(IF=2.78) https://doi.org/10.1061/(ASCE)GM.1943-5622.0001920.

[29] Deendayal Rathod, K.T. Krishnanunni and D. Nigitha: A Review on conventional and innovative pile system for offshore wind turbines, *Geotechnical and Geological Engineering,*

243